Macromolecular Rapid Communications
www.mrc-journal.de

Circularly Polarized Light-Driven Supramolecular Chirality

Jun Su Kang, Namhee Kim, Taehyung Kim, Myungeun Seo, and Byeong-Su Kim**

Introduction of asymmetry into a supramolecular system via external chiral stimuli can contribute to the understanding of the intriguing homochirality found in nature. Circularly polarized light (CPL) is regarded as a chiral physical force with right- or left-handedness. It can induce and modulate supramolecular chirality due to preferential interaction with one enantiomer. Herein, this review focuses on the photon-to-matter chirality transfer mechanisms at the supramolecular level. Thus, asymmetric photochemical reactions are reviewed, and the creation of a chiral bias upon CPL irradiation is discussed. Furthermore, the possible mechanisms for the amplification and propagation of the bias into the supramolecular level are outlined based on the nature of the photochromic building block. Representative examples, including azobenzene derivatives, polydiacetylene, bicyclic ketone, polyfluorenes, C_n-symmetric molecules, and inorganic nanomaterials, are presented.

1. Introduction

The origin of biological homochirality, such as L-amino acids and D-mononucleotides, has attracted significant attention from scientists because it induces specific steric structures and functions in biological processes.[1–3] Proteins and nucleic acids as helical assemblies, which are assembled via noncovalent interactions between each repeating molecular units, are ubiquitously found in nature, and they are fundamental in determining the activities of biological materials. Inspired by these unique features found in nature, the transfer of chiral information from molecular to macroscopic level by developing artificial self-assembly systems mimicking natural self-assemblies has garnered considerable interest.[4–6]

J. S. Kang, M. Seo
Department of Chemistry
Korea Advanced Institute of Science and Technology (KAIST)
Daejeon 34141, Republic of Korea
E-mail: seomyungeun@kaist.ac.kr

N. Kim, T. Kim, B.-S. Kim
Department of Chemistry
Yonsei University
Seoul 03722, Republic of Korea
E-mail: bskim19@yonsei.ac.kr

T. Kim
Department of Energy Engineering
Ulsan National Institute of Science and Technology (UNIST)
Ulsan 44919, Republic of Korea

The ORCID identification number(s) for the author(s) of this article can be found under https://doi.org/10.1002/marc.202100649

DOI: 10.1002/marc.202100649

In 1995, Green et al. reported that the essential characteristics for yielding elegant chiral structures are readily interconvertible chiral senses between molecular and supramolecular structures.[7] Thereafter, the formation process of supramolecular structures has been studied to determine the interaction mechanism between molecular structures. Several studies have reported that the control of noncovalent interactions, such as hydrogen bonding, π–π stacking, van der Waals interaction, hydrophobic interaction, and electrostatic interaction, is critical for obtaining well-organized self-assemblies. Moreover, the size and structure of supramolecular assemblies with reversible noncovalent interactions are primarily governed by external environment, such as solvent,[8,9] temperature,[10,11] light,[12,13] and metal ions.[13,14]

In biological compounds, high optical purity is essential for acquiring supramolecular helical assemblies. Furthermore, supramolecular helical structures have been constructed through intrinsic molecular design and external stimuli. Molecular chirality, such as point, axial, and helical chirality, causes the helicity of supramolecular assemblies. Additionally, due to the dynamic noncovalent bonding, it offers a promising strategy for using external stimuli to induce and modulate the macroscopic helicity of supramolecular assemblies. Among the various external stimuli,[15] light is widely used as a nondestructive stimuli in supramolecular chiral systems due to its facile processing, high spatiotemporal control, and fast read-out.[16] Based on the one-handed helical arrangements, the induced macroscopic chirality of supramolecular assemblies can be applied to the efficient separation of enantiomers,[17–21] chiral recognition,[22,23] and asymmetric catalysis.[24–26]

Particularly, circularly polarized light (CPL) is regarded as a representative chiral physical force.[27,28] It has been extensively applied in asymmetric photochemical processes to impart initial chiral bias. The anisotropy factor ($g = \Delta\epsilon/\epsilon$) is essential for determining the enantiomeric excess (*ee*) of chiral products in such asymmetric photochemical reactions; it is the ratio between the molar circular dichroism ($\Delta\epsilon = \epsilon_{l\text{-CPL}} - \epsilon_{r\text{-CPL}}$) and the molar absorption coefficient ($\epsilon = (\epsilon_{l\text{-CPL}} + \epsilon_{r\text{-CPL}})/2$). Thus, a high anisotropy factor yields a high *ee* value for enantioselective reactions. In other words, the interaction between CPL and molecules and supramolecular assemblies is sensitive to molecular chirality.

Under CPL irradiation, prochiral molecules can preferentially convert ground states to excited states, forming an enantiomer with a certain chirality. Stereoregular packing/polymerization

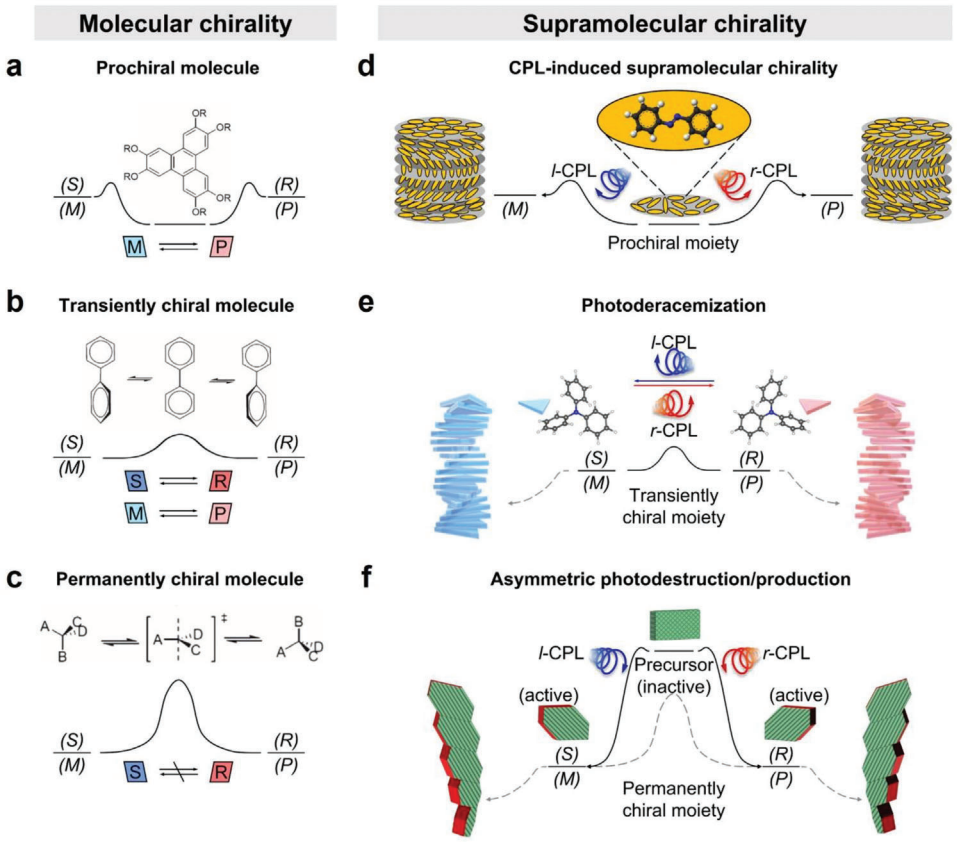

Scheme 1. Schematic representation of the chirality induction and modulation at the a–c) molecular and d–f) supramolecular levels, and the potential energy diagrams of enantiomerization for each case. At the molecular level, a) prochiral molecules with the lowest energy achiral conformer and b) transiently chiral molecules can be in equilibrium with their enantiomers due to their relatively low energy barrier for enantiomerization. c) Because permanently chiral molecules have a sufficiently high energy barrier, enantiomerization cannot occur between their enantiomers. Reproduced with permission.[67] Copyright 2015, Wiley-VCH GmbH. d) Prochiral, e) transiently chiral, and f) permanently chiral building blocks with circular dichroic properties can undergo symmetry breaking via CPL-induced enantioselective photochemical reactions. Then, the resulting chiral bias is transferred and amplified to the supramolecular level via the self-assembly process.

is primarily produced by the photoinduced process at the supramolecular level. That is, the CPL absorption from chiral molecules can afford a slight bias in an enantiomer and cause preferential resolution or destruction. Therefore, CPL can be employed to distinguish the optical isomers of chiral molecules via differences in molar extinction coefficients between right-handed CPL (*r*-CPL) and left-handed CPL (*l*-CPL), called the photoresolution effect. Moreover, CPL can participate in irreversible photodestructive processes, resulting in symmetry breaking wherein an enantiomer in a racemic mixture is preferentially eliminated, while the other enantiomer is concentrated. The resulting chiral bias can be amplified to the supramolecular level by enantioselective association, affording a predominant helical sense. Conversely, the chiral bias can be transmitted to another achiral molecule, and it causes helical arrangement in the chirality induction mechanism. **Scheme 1** illustrates the possible symmetry breaking scenarios at the molecular level upon CPL irradiation and amplification of the chiral bias into the supramolecular level.

Although there are many outstanding reviews about the chirality of supramolecular assemblies induced and modulated by external stimuli,[29–33] only a few reviews have focused on the enantiospecific process of supramolecular assemblies promoted by CPL irradiations.[16,28] Therefore, herein, we review the mechanisms of CPL-induced enantioselective processes at the supramolecular level by classifying them into three types: stereoregular packing/polymerization, photoderacemization, and asymmetric photodestruction/production. We aim to clarify the mechanism of photon-to-matter chirality transfer for each subset by commencing from the photochemical interaction of the building blocks with CPL from the molecular perspective to create a chiral bias. Furthermore, possible routes for amplification of the asymmetry are illustrated along with the discussion with representative examples from the mechanistic perspective.

2. Stereoregular Packing/Polymerization

As achiral conformers, prochiral molecules possess a ground state with minimal energy, but they can easily transform into chiral conformers (**Figure 1**a). This is the asymmetric photosynthesis; it induces the enantioselective photochemical reaction of an optically active compound.[34] Prochiral molecules can preferentially convert a ground state into an exited state with a certain chirality by a slight twist under CPL irradiation, yielding an enantiomer.

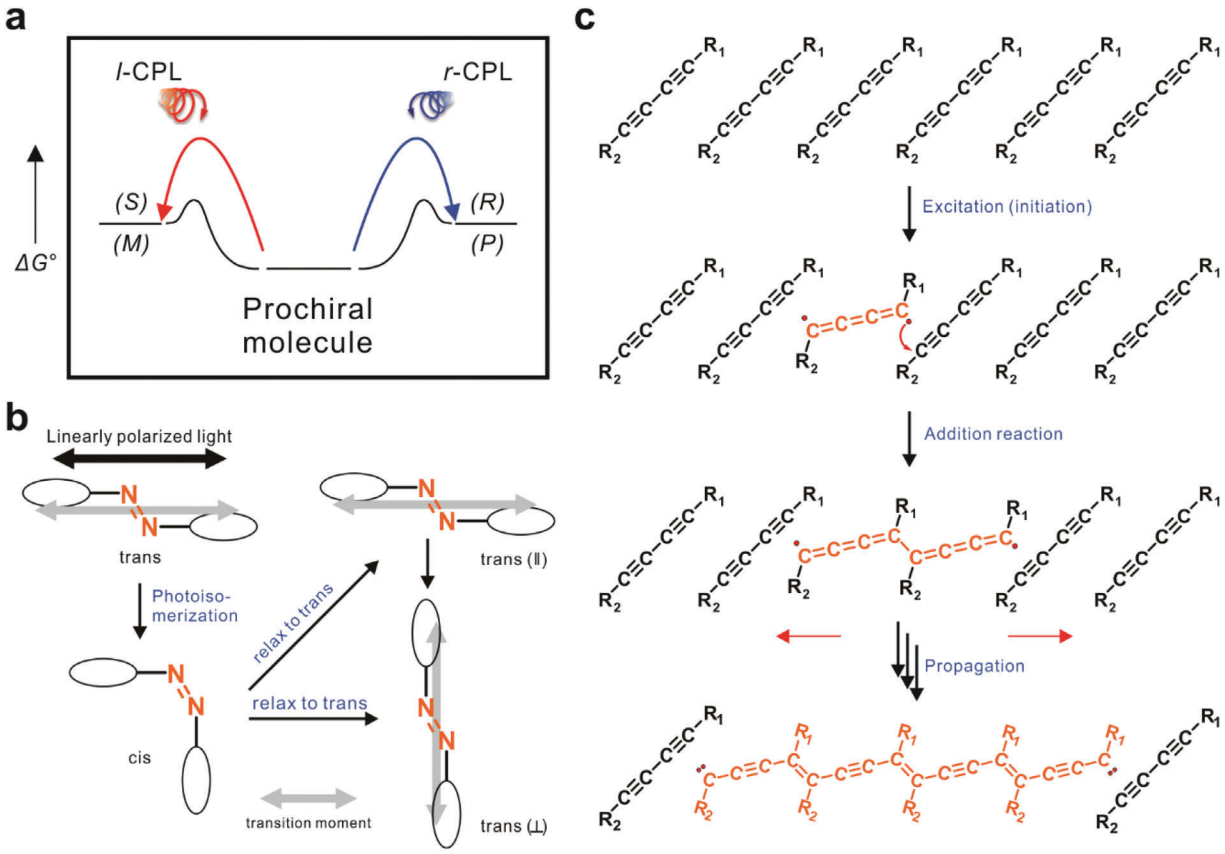

Figure 1. a) Energy diagram of the CPL-induced stereoregular packing/polymerization of prochiral molecules. b) Azobenzene chromophore and CPL interaction mechanism. Reproduced with permission.[35] Copyright 2007, The Royal Society of Chemistry. c) Photopolymerization mechanism of polydiacetylene. Reproduced with permission.[36] Copyright 2012, The Royal Society of Chemistry.

Azobenzene derivatives, as representative prochiral molecules, can be self-assembled via π–π^* stacking between azobenzene groups or between adjacent phenyl groups. Additionally, azobenzene chromophores exhibit unique photoresponsive properties, such as photoinduced isomerization, that induce efficient coupling of CPL to the molecules (Figure 1b). Moreover, polydiacetylene (PDA) is usually synthesized via the solid-state photopolymerization of prochiral diacetylene (DA) monomers with diradical formation under UV irradiation (Figure 1c). This polymerization condition affords enantioselective PDA under CPL irradiation. After the enantiomeric state with specific handedness is enriched by CPL, the chiral bias can be amplified and fixed via self-assembly or polymerization processes (**Scheme 2**). The representative examples of supramolecular chirality via stereoregular packing/polymerization are organized in **Table 1**.

2.1. Azobenzene in Side Chain

This section introduces the phenomena of CPL-induced chirality of azobenzene chromophores located either in the side chain or main backbone. In side-chain systems, the aggregation of achiral azobenzene groups leads to superstructural chiral properties, such as helical structures. In contrast, in main backbone systems, macroscopically induced chirality can occur in the chirality of each azobenzene chromophore in the backbone.

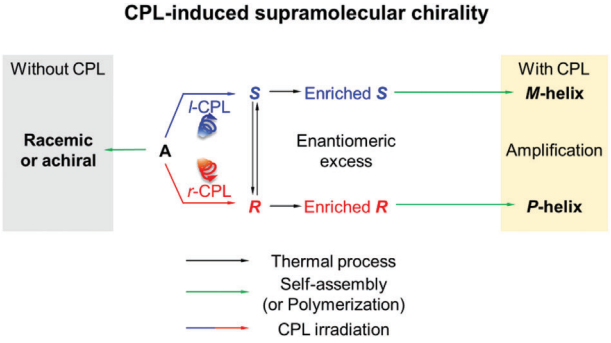

Scheme 2. Schematic illustration of the CPL-induced supramolecular chirality. An enantiomeric form can be enriched upon CPL exposure to a prochiral building block (**A**) through asymmetric photochemical reactions. The chiral bias can be amplified to the supramolecular level via self-assembly or polymerization processes. While the mirror-imaged isomers produce the mirror-imaged helices such as *S*-enatiomer to *M*-helix and *R*-enatiomer to *P*-helix or vice versa, only one case was illustrated for clarity. It is also of note that the morphology of supramolecular chirality is not necessarily a helical structure. Here, *M*- and *P*-helixes are presented as a representative example.

Azobenzene chromophores have attracted significant attention due to the photoinduced changes via the *trans–cis* isomerization cycle of photochromic bonds (**Figure 2**a).[41–44] A notable feature is the photoalignment of azobenzene molecules

Table 1. Representative examples of supramolecular chirality via stereoregular packing/polymerization.

Chromophore	Position	Features	Morphology	Absorption wavelength	Intensity	Ref.
Azobenzene	Side chain	– Main chain: polymethacrylate – Reversible chiroptical switching	LC film	514 nm	75 mW cm^{-2}	[38]
		– Main chain: polyether	Amorphous film	488 nm	100 mW cm^{-2}	[39]
		– Main chain: polymethacrylate – Circular Bragg reflection	LC film	458, 488, or 514 nm	120 mW cm^{-2}	[91]
		– Main chain: polymethacrylate – Reversible chiroptical switching – Circular Bragg reflection	LC film	488 nm	120 mW cm^{-2}	[92]
		– Main chain: polymethacrylate – Circular Bragg reflection	LC film	488 nm	20 mW cm^{-2}	[93]
		– Main chain: polymethacrylate – Reversible chiroptical switching – Circular Bragg reflection	LC film	488 nm	20 mW cm^{-2}	[94]
		– Main chain: polymethacrylate – Reversible chiroptical switching – CPL wavelength-dependent chirality	DCE/MCH solution	313, 365, 405, or 436 nm	0.03 mW cm^{-2}	[40]
	Main chain	– Bent-shaped mesogen	LC film	365 nm	0.03 mW cm^{-2}	[53]
		– Polyazourea – Reversible chiroptical switching	Amorphous film	442 nm	30 mW cm^{-2}	[54]
		– W-shaped molecule – Reversible chiroptical switching	LC film	365 nm	30 mW cm^{-2}	[55]
Acetylene	Main chain	– Side chain: alkyl chain	LB Film	314 nm	19.4 mW cm^{-2}	[62]
		– Side chain: azobenzene	LB Film	313 nm[a] 520 nm[b]		[63]
		– Side chain: azobenzene – Reversible chiroptical and thermal switching	LB Film	313 nm[a] 442 nm[b]	19.4 mW cm^{-2}	[58]
		– Side chain: azobenzene – Linear (DA1), hydoxyl substitution (DA2), two diacetylene chain (DA3)	LB Film	313 nm[a] 365 nm[b] 435 nm[b]		[95]
		– Circularly polarized visible light – Excited PDA oligomer with carbene radicals (cf. UV excited monomer with biradicals)	Film	523 nm[a] 254 nm[c]	30 mW cm^{-2}	[60]
		– Side chain: carboxylic acid and alkyl chain – Hydrogen bonding assembly – Alignment after thermal treatment before polymerization under CPUL	LC film	313 nm	19 mW cm^{-2}	[59]
		– Side chain: alkyl chain – Selective adsorption of one-handed CPL in LPL under magnetic field	LC film	313 nm[d]	20 mW cm^{-2}	[65]
		– Side chain: benzaldehyde and alkyl chain – Dissymmetry enhancement by superchiral light	LB Film	325 nm	4.0 and 2.8 mW cm^{-2}	[64]

[a] Wavelength of CPL for polymerization; [b] Wavelength of CPL for switching chirality; [c] Wavelength of UV light for initiation; [d] Wavelength of LPL with magnetic field 0.5 T.

by linearly polarized light (LPL), referred to as the Weigert effect.[30,35,45,46] *Trans*-azobenzene molecules with transition moments parallel to the polarization direction of LPL are excited to *cis*-azobenzene molecules via *trans–cis* isomerization and then relaxed to *trans*-azobenzene molecules that are aligned perpendicular to the LPL direction. After multicycles of *trans–cis* isomerization, azobenzene molecules with transition moments perpendicular to the polarization direction are dominate. In summary, the stereoregular packing of photoresponsive materials with the azobenzene groups in the side chain and main backbone is induced via the *trans–cis* isomerization of azobenzene molecules.

Nikolova et al. were the first to display the photoinduced optical activity of amorphous films and liquid crystals (LCs) containing azobenzene molecules in the side chain.[47,48] Thereafter, the photoinduced chiroptical properties of the achiral azobenzene chromophores have been widely studied.[49–52] For example, Iftime et al. reported that liquid crystalline methacrylic polymers with the azobenzene molecules in the side chain induced chiral properties via CPL irradiation (Figure 2b).[38] Moreover, in their

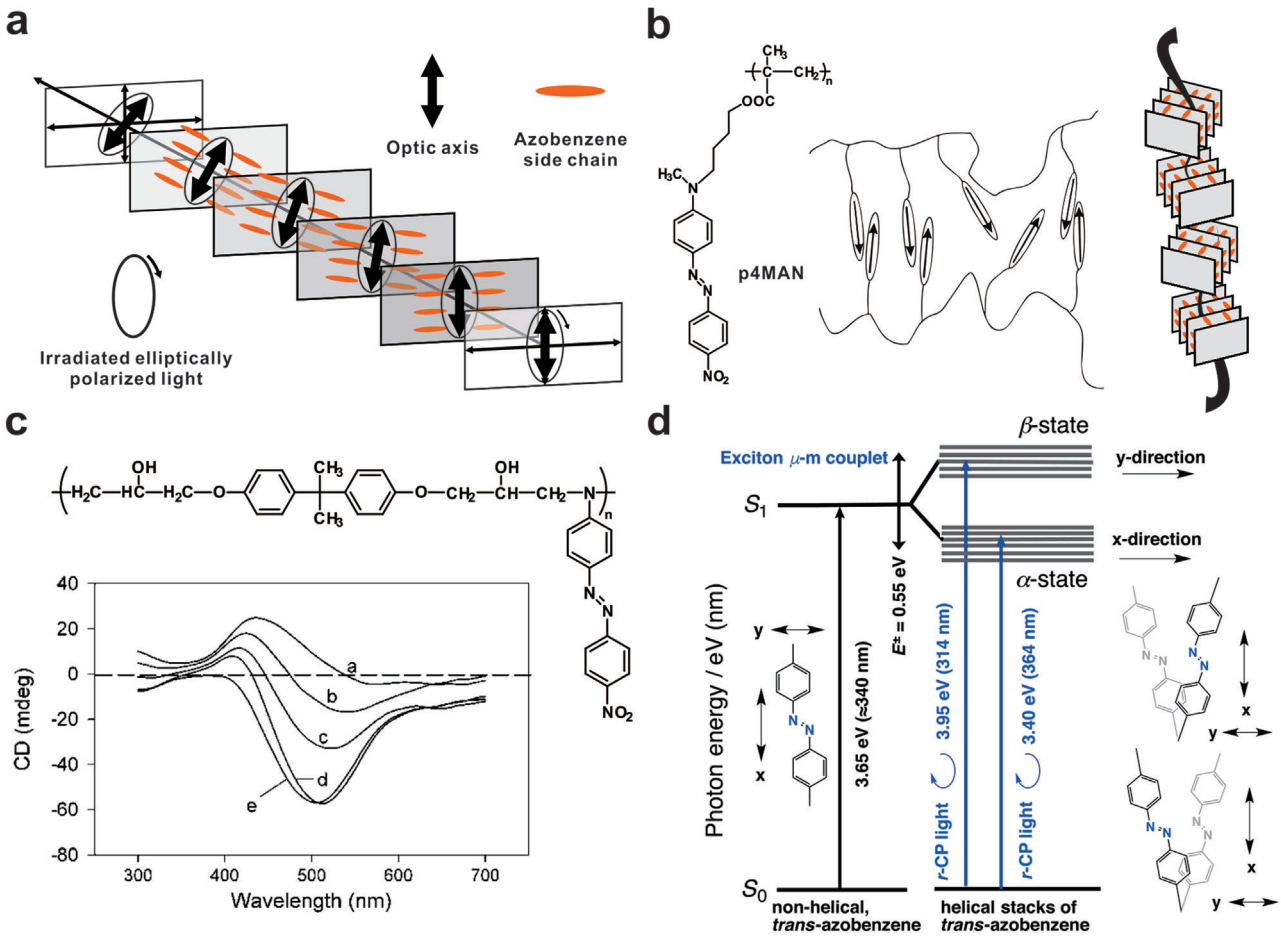

Figure 2. a) Schematic of the mechanism for the formation of the helical structure of a side-chain azopolymer film induced by elliptically polarized light. Reproduced under terms of the CC-BY license.[37] Copyright 2020, the Authors. Published by MDPI. b) The helical arrangement of azobenzene liquid crystalline polymer (p4MAN) produced by irradiation with CPL. Reproduced with permission.[38] Copyright 2000, American Chemical Society. c) Chemical structure and CPL-induced circular dichroism (CD) spectra of epoxy-based amorphous polymer films. Reproduced with permission.[39] Copyright 2002, American Chemical Society. d) Jablonski diagram of the twisted azobenzene stacks with chiroptical switching properties under wavelength-dependent irradiation. Reproduced with permission.[40] Copyright 2017, American Chemical Society.

study, CPL irradiation with opposite handedness afforded enantiomeric structures. The *l*- and *r*-CPL exhibited left- and right-handed helical supramolecular structures, respectively. In contrast, non-annealed amorphous films did not exhibit any circular anisotropy, suggesting that the photoinduced helical structure is induced by the azobenzene groups in liquid crystalline arrangement. They also proposed that photoisomerization converted the original CPL into an elliptical state by the first layer of the thin film and the azobenzene molecules were angularly reoriented in all directions with the same probability. Thus, the second layer was irradiated by a beam with elliptical polarization, producing a new optical axis. Because the angular reorientation of the azobenzene moieties depends on polarization, the polymer backbone connected to the photoactive azobenzene molecules can be moved. Further, photoisomerization and angular reorientation were extended along successive layers through a stepwise process, forming a planar twist-grain-boundary-like phase. Because the backbones are mainly present in the smectic layers and the azobenzene groups in the side chain are located between the smectic grains, a chirality of the main chain was induced. Notably, a reversible chiroptical property between two chiral supramolecular structures was reported in this study.

The chiral orientation in an amorphous polymer film bearing azobenzene chromophores is derived similar to that in cholesteric LCs. Kim et al. revealed CPL-induced chirality for amorphous azobenzene polymeric films (Figure 2c).[39] Therein, liquid crystallinity was not a prerequisite for CPL-induced chiral properties. Epoxy-based azobenzene polymers were used as amorphous films. No CD signals from the unirradiated films were observed, implying that the films were initially achiral. When the films were irradiated with *l*- and *r*-CPL, no CD signal was also observed; however, a large CD signal was detected after LPL was introduced to the incident CPL to produce an elliptically polarized light (EPL). The results showed that the chiral orientation of azobenzene molecules in amorphous polymeric films can be optically induced using a combination of LPL and CPL. Thus, the stepwise rotation of azobenzene molecules along the light propagation yields chiral structures.

In another study, Wang et al. determined that the chiroptical properties of polymethacrylate systems with azobenzene groups

relied on CPL sources with multiple wavelengths (Figure 2d).[40] Additionally, the bisignate Cotton effect of azobenzene polymers was enhanced under *l*- and *r*-CPL (365 nm) irradiation, affording intense couplets at the π–π^* transitions of the CD spectra. The highest dissymmetry ratio (g_{CD}) of aggregates irradiated by CPL source at 365 nm was $\approx\pm 1.0 \times 10^{-2}$ at 313 nm. Furthermore, the CPL-wavelength-dependent switching of induced chirality was observed in multiple cycles after CPL irradiation. When samples were irradiated with *l*-CPL of 436 nm, negative and positive signals were observed at 390 (first Cotton band) and 310 nm (second Cotton band), respectively. In contrast, upon irradiation with *r*-CPL of 436 nm, positive and negative signals were observed at 390 and 310 nm, respectively. However, the CD signal of the azobenzene aggregates completely reversed after irradiation with *r*-CPL of 313 nm. Wang et al. further suggested that selective *x*- and *y*-axis responses induced by optomechanical torque could result in twisted azobenzene moieties with CPL-wavelength-dependent chiroptical properties. Moreover, they demonstrated the high resistance of chiroptical activity in the dark for over one week by retaining this switching process over several cycles.

Most studies explain the chiroptical properties induced by CPL as a mechanism for transferring the angular momentum from CPL to azobenzene chromophores. Nikolova et al. proposed a detailed mechanism of interaction between the azobenzene groups and incident CPL.[48] *r*-CPL excites azobenzene chromophores, followed by multiple *trans–cis* isomerization. The resultant *trans* isomers tend to reorient perpendicular to the light polarization direction, leading to an anisotropic state with an optical axis. After the formation of the anisotropic state, CPL decomposes into two LPLs with Eigenmodes. The amplitude and phase difference between the two LPLs vary during light propagation due to the anisotropic refractive index of each layer. Consequently, the propagating light through the film forms an optical axis that rotates along the thickness of each layer.

2.2. Azobenzene in Main Chain

Although the mobility of azobenzene groups in the main chain is limited due to its low degree of freedom, the polymer backbone still provides sufficient flexibility for the alignment of azobenzene moieties in the main chain (**Figure 3**a). Choi et al. introduced CPL-induced chirality of bent-shaped dimeric compounds, which are representative of main-chain-type polymers, wherein two azobenzene moieties are linked by a polymethylene group (Figure 3b).[53] They used a phase sequence of isotropic-(108 °C)-SmCA-(94 °C)-B4. Microscopically chiral segregation spontaneously occurred in the B4 phase with the lowest temperature. The large CD signals at ≈380 nm were generated by CPL irradiation, affording positive and negative signals via *l*-CPL and *r*-CPL, respectively. In contrast, no CD signal was observed without CPL irradiation because the ratio of the positive and negative domains was about 50:50, implying that two chiral conformers with equal probability exist.

The origin of the chirality induced in the B4 phase was confirmed via nuclear magnetic resonance (NMR) measurements and molecular calculations.[56] The NMR spectra confirmed the presence of racemic mixture with twisted conformation: the molecules did not possess any asymmetric carbon. Molecular calculations indicated that the most stable conformers are twisted, comprising both (+) and (−) conformers. After CPL irradiation, one of the two chiral conformers becomes preferential due to the absorption differences between *l*-CPL and *r*-CPL, which unbalances the energy of ground states.

Moreover, CPL-induced chirality has been demonstrated in polymer systems with the azobenzene groups in the main chain (Figure 3c).[54] Therein, the absorption maximum (λ_{max}) of an amorphous polyazourea thin film with high glass-transition temperature (T_g) was observed at ≈400 nm. The 442-nm He-Cd laser was an effective light source for chiral induction as it excited the π–π^* band of azobenzene groups. When the intrinsic achiral polymer film was irradiated with *l*- or *r*-CPL, CD peaks with opposite handedness were observed at about 422 nm in the CD spectrum. The CD peak intensity was enhanced by increasing the CPL irradiation time. The mirror images in the CD spectrum were similar to those in the polymer systems containing azobenzene moieties in the side chain. In addition, CPL was alternatively irradiated to demonstrate the possibility of chiral modulation for polyazourea films. The chiroptical signal at 442 nm in the CD spectrum was actually switched under alternating *l*- or *r*-CPL irradiations for 30 min. The results showed that the azobenzene chromophores in the polymer backbone were consistently active on CPL.

Choi et al. reported the CPL-induced chirality of W-molecule-doped polymeric LC films with two main-chain azobenzene groups (Figure 3d).[55] The film afforded after the doping of W-shaped azobenzene molecules into the intrinsic achiral film exhibited photoresponsive properties under irradiation with CPL. The irradiation with *l*- or *r*-CPL at 365 nm revealed the CD profiles with opposite signs. Furthermore, the chiral modulation phenomenon was observed under alternating CPL irradiation with opposite handedness. Interestingly, the CD spectra of the twisted conformation were simulated using the coupled oscillator approach. The theoretically calculated CD spectra agreed well with that observed experimentally. Choi et al. also proposed a mechanism for the CPL-induced chirality of the W-molecule-doped main-chain LC film. One enantiomer with a negligibly small net excess in the W-doped film afforded a racemic state, while the twisted conformation of W-shaped molecules afforded a chiral state with opposite handedness. For *r*-CPL irradiation, the angular momentum was transferred from *r*-CPL to W-shaped molecules because the incident beam rotated the electric field direction to the right. Therefore, the net population of W-shaped molecules with right-twisted conformation increased, causing the macroscopic-handedness chirality in the prepared films. Similarly, *l*-CPL irradiation increased the net population of left-twisted W-shaped molecules.

Additionally, CPL irradiation induced the free volume in the polymer backbone and transformed the initial polymer backbone into the perturbation state due to the photoisomerization of the W-shaped molecules containing two azobenzene groups in the main chain. Therefore, their conformation and/or orientation can be easily transformed into the preferred twisted conformation. Such a reorientation is possible due to the local heating caused by the light absorption of polymers with low T_g.

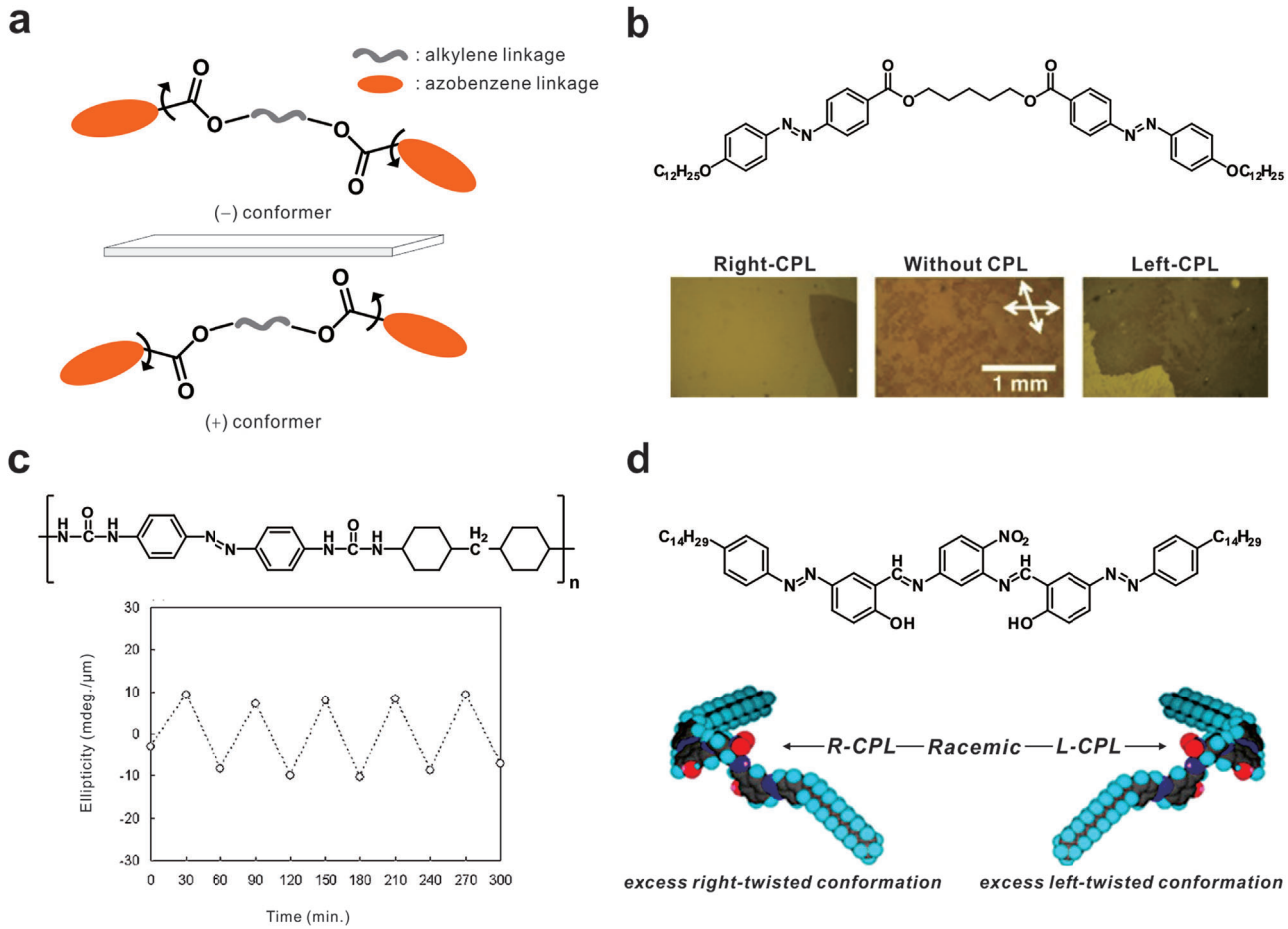

Figure 3. a) Schematic illustration for the formation of the helical structure of main-chain azobenzene by CPL irradiation. Reproduced with permission.[35] Copyright 2007, The Royal Society of Chemistry. b) Optical microscopy images with and without CPL treatment of an achiral, bent-shaped mesogen. Reproduced with permission.[53] Copyright 2006, Wiley-VCH GmbH. c) Chemical structure and absorption spectrum of polyazourea with chiroptical modulating property at 422 nm by alternating *l*- and *r*-CPL irradiations. Reproduced with permission.[54] Copyright 2006, The Japan Society of Applied Physics. d) The most stable twisted conformation of the W-shaped azobenzene molecule. Reproduced with permission.[55] Copyright 2006, American Physical Society.

2.3. Polydiacetylene

This section presents the solid-state polymerization of enantioselective PDA induced by CPL irradiation from a Langmuir–Blodgett (LB) film to LC phase. PDA is a well-known π-conjugated polymer that is widely used in the optical, electrical, and biomedical materials.[61] PDA is commonly synthesized via photopolymerization under UV or γ irradiation, which afford high purity PDA without byproducts. When circularly polarized ultraviolet light (CPUL) was used instead of nonpolarized light, one-handed enantioselective polymerization occurred (**Figure 4**a). Manaka et al. proposed the enantioselective polymerization mechanism based on the interaction between CPUL and diacetylene monomers.[62] Because the photoexcitation of two diacetylene monomers is important at initial stage of PDA formation, the interaction between the CPL and the diacetylene dimer plays a vital role in the enantioselective polymerization of PDA. Moreover, the crowded packing of the aliphatic chain slightly distorted the arrangement of the PDA backbone, thus maintaining the chiral structure of PDA after polymerization.

Furthermore, to explore the relationship between the side functional group and enantioselective polymerization, Zou et al. introduced an azobenzene moiety as a side functional group in the PDA structure (Figure 4b).[58,63] The overcrowded array of azobenzene moieties during the vacuum-assisted film formation plays a dominant role in the formation of enantiomeric helical PDA chains. Although chiroptical switching was not realized in the alkyl-substituted PDA, the azobenzene-functionalized PDA exhibited reversible chiroptical switching due to the photoinduced rearrangement property of azobenzene chromophores. In addition, the heating and cooling cycles from room temperature to 80 °C provide reversible switching between left- and right-handed helicity.

Unlike the abovementioned LB film example, Xu et al. demonstrated the synthesis of helical PDA in the LC phase (Figure 4c).[59] The LC state developed by the hydrogen bonding complex formation and self-assembly transformed to lamellar columnar mesophase (L_{Col}). Interestingly, L_{Col} only formed helical PDA under CPUL irradiation due to the relatively free molecular motion that aligned diacetylene units in a suitable helical

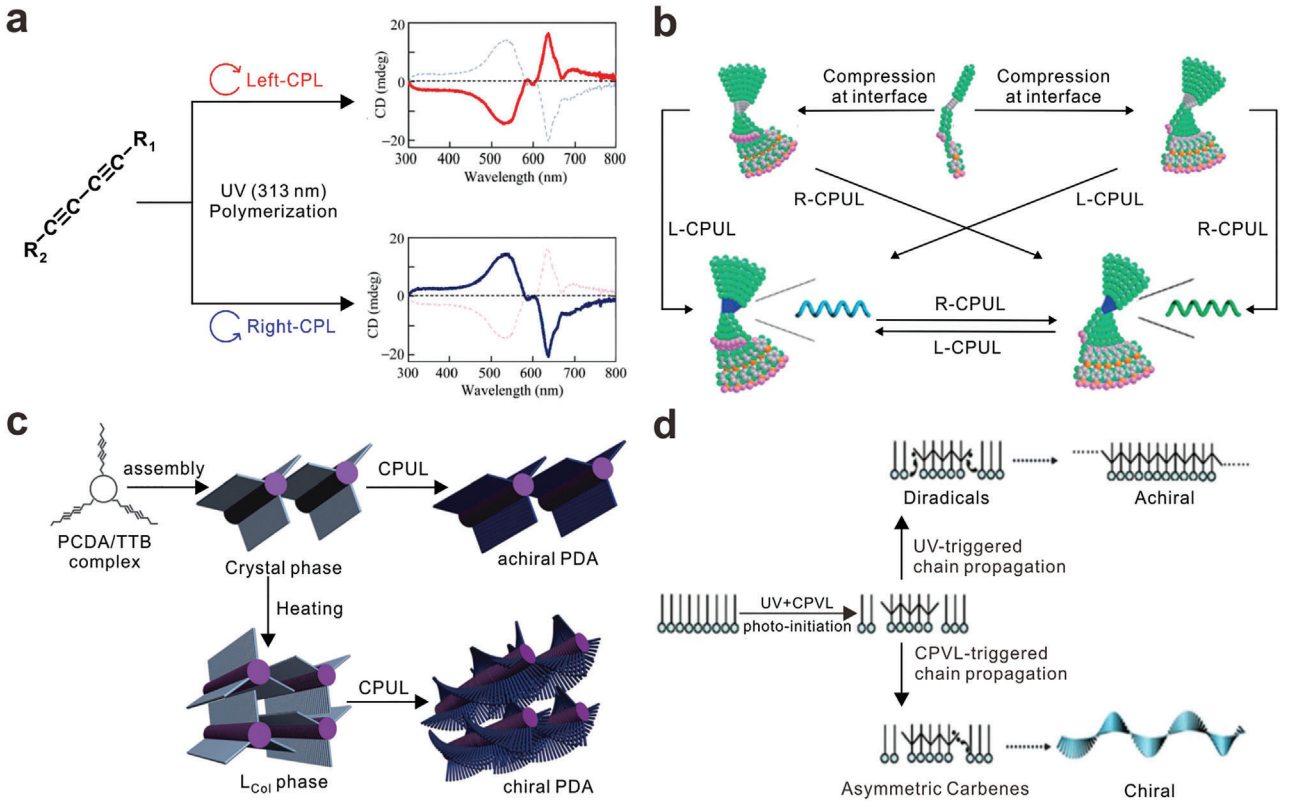

Figure 4. a) Preparation of chiral PDA films upon *l*- or *r*-CPL irradiation. Reproduced under terms of the CC-BY license.[57] Copyright 2019, the Authors. Published by MDPI. b) Schematic representation of the chiral induction and modulation with CPL irradiation. Reproduced with permission.[58] Copyright 2010, The Royal Society of Chemistry. c) Schematic representation of the formation mechanism of helical PDA films in the L_{col} LC state. Reproduced with permission.[59] Copyright 2014, The Royal Society of Chemistry. d) Schematic representation of the enantioselective polymerization by circularly polarized visible light. Reproduced with permission.[60] Copyright 2014, The Royal Society of Chemistry.

orientation. However, molecular motion in the crystal phase was restricted by the crystal lattice, and diacetylene units could not be aligned in a suitable helical orientation. As a result, helical PDA can be synthesized in the LC phase when it contains the proper molecular motion.

While previous studies demonstrated the enantioselective synthesis of PDA under CPUL, Yang et al. demonstrated that chiral PDA can be synthesized under circularly polarized visible light (CPVL) irradiation (Figure 4d).[60] Because the essential excitation energy decreases with increasing active PDA chains, visible light can synthesize PDA when the number of repeating units is more than five. When they simultaneously irradiated unpolarized UV light and CPVL, the unpolarized UV light excited diacetylene monomers and initiated the polymerization of DA monomers and CPVL propagated the PDA chain enantioselectively.

Most previous studies consider the enantioselective polymerization induced by CPL irradiation as the interaction mechanism between CPL and diacetylene dimer with the appropriate alignment for the reaction between the dimer molecules. Because two diacetylene monomers are photoexcited at the initial stage of PDA formation, the enantioselective polymerization of PDA is directly based on the interaction between CPL and the diacetylene dimer. Furthermore, the close and ordered packing is important as chiral transfer occurs during the 1,4-addition in PDA polymerization.

In addition to the aforementioned examples of chiral PDAs, recent studies expanded the induction of chirality in PDA by not only amplification of the chirality during the synthesis of chiral PDA but also synthesis of chiral PDA using LPL under the magnetic field. He et al. reported the dissymmetry enhancement of chiral PDA using superchiral light (SCL) during asymmetric polymerization (**Figure 5**a).[64] SCL was generated by the interference of two counter-propagating CPL beams with the same frequency, opposite handedness, and slightly different intensities. The SCL-induced chiral PDA exhibited enantioselective colorimetric responses that can be applied as visual sensors for chiral molecule detection.

As a unique example, Xu et al. demonstrated that the enantioselective polymerization of diacetylene derivatives can be achieved in the LC phase with LPL irradiation in a parallel magnetic field (Figure 5b).[65] During the photoinitiation of polymerization with the biradical mechanism, diacetylene monomers preferentially absorbed one-handed CPL from LPL due to the magnetochiral dichroism effect. Thus, it was suggested that enantioselective photopolymerization can be achieved via LPL irradiation in the presence of a magnetic field. In summary, chirality amplification using CPL and induction using LPL was successfully

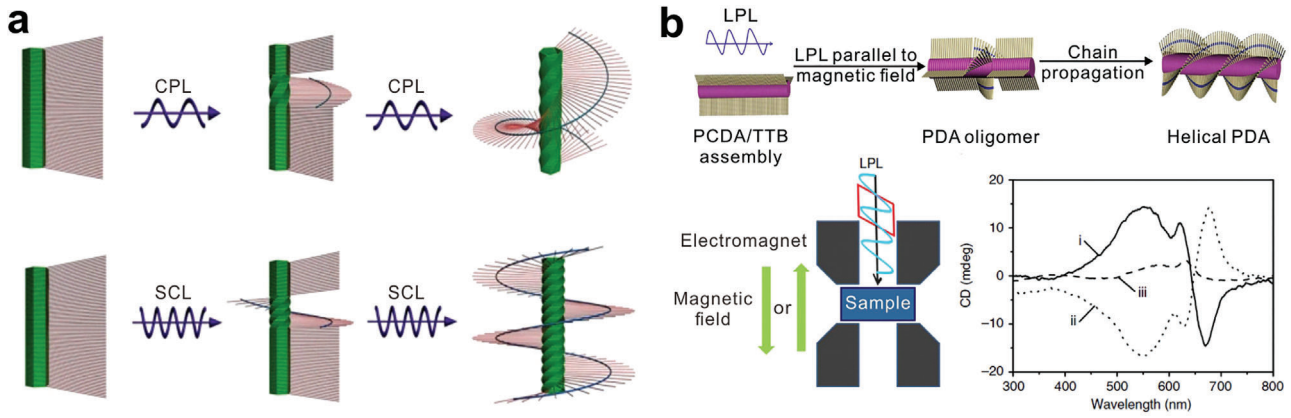

Figure 5. a) Schematic representation for the asymmetric photopolymerization mechanism for helical PDA chains prepared via CPL and SCL irradiation. Reproduced under terms of the CC-BY license.[64] Copyright 2018, the Authors. Published by Springer Nature. b) Schematic representation of the asymmetric polymerization mechanism for the HB complex samples prepared via LPL irradiation, and the magnetic field parallel to the irradiation direction with the experimental setup scheme and CD spectra of PDA films. Reproduced with permission.[65] Copyright 2014, Springer Nature.

demonstrated based on the electromagnetic wave properties (i.e., wave interference and interaction with magnetic field) in the synthesis of helical PDA through polarized light irradiation.

3. Supramolecular Chirality via Photoderacemization

Compared to the prochiral azobenzene and diacetylene moieties discussed above, transiently and permanently chiral motifs possess stable *R*- and *S*-configurations as global minima separated by the enantiomerization barrier (Scheme 1b,c). Irradiation of the racemic mixture with CPL at an appropriate wavelength can induce symmetry breaking via the enantiomerization reaction; it may require the rotation of substituents in the motif or the breaking of a bond. **Scheme 3**a schematically depicts a possible scenario, called photoderacemization (partial photoresolution), where chiral conformers in the ground state in absence of light cannot isomerize into the opposite conformation.[34,66] Upon CPL exposure, each conformer absorbs different extents of CPL depending on the CPL handedness because of the unequal molecular extinction coefficients ϵ, affording enantioselective excitation.

In the depicted adiabatic condition, excited conformers can be directly interconverted. The mixture eventually restores the entropically favored racemic state when CPL is turned off. However, the asymmetric population may propagate into the supramolecular level if the conformation is retained upon relaxation and fixed in the assembled state. Assuming enantiophobic interaction, steric congestion and noncovalent interaction between neighboring units promotes the assembly of conformers with the same chirality, which causes self-sorting.[67] Thus, in contrast to the formation of racemic conglomerate in the absence of CPL, CPL-enriched conformers determine the direction of the net supramolecular chirality. Chirality can be further amplified to the supramolecular level when the system follows the majority rule, suggesting that a chirality-mismatching conformer is forced to adopt the conformation determined by the supramolecular chirality of the assembly, e.g., helical sense, to avoid helix reversal.[68] If the conformation is "unfixed" (i.e., by raising the temperature or irradiating with non-polarized light/LPL), reversible control of the supramolecular chirality would be possible with CPL.

Scheme 3b illustrates another possible route for transmitting chiral information of CPL into supramolecular assemblies through photoderacemization-driven chirality induction. Here, the enriched chiral conformer produced by the photoderacemization reaction interacts with another achiral molecule and induces supramolecular chirality. This is similar to the sergeants-and-soldiers principle, wherein supramolecular chirality emerges from the co-assembly of a sergeant molecule possessing permanent chirality with achiral soldier molecules.[68]

In this section, we discuss the different classes of photoresponsive systems where supramolecular chirality stems from asymmetric photochemical reactions. To our knowledge, although several photoderacemization-based systems have been reported, studies utilizing photodestruction/production are rare. Nonetheless, a few recent studies on chiral inorganic nanostructures and chiral polymerization appear promising. The representative examples of supramolecular chirality via photoderacemization are summarized in **Table 2**.

3.1. Bicyclic Ketones

In 1995, Zhang and Schuster reported the first example of the reversible photoresolution of bicyclic ketone-containing compounds upon CPL irradiation. They examined the reversible photoderacemization of bicyclooctan-3-one derivatives possessing axial chirality with CPL (**Figure 6**a).[69] To increase the *g* factor, a small extinction coefficient corresponding to the forbidden n–π^* transition of the ketone group and high $\Delta\epsilon$ values from the twisted ketone conformation in the rigid bicyclic framework were used. When an olefinic double bond was installed on the opposite side of the framework, the intramolecular triplet–triplet energy transfer from the ketone to the olefin allowed the interconversion of axially chiral conformers. These molecules generally exhibit high quantum yields for photoracemization (Figure 6b).[69,70,72] Upon exposure to *l*- and *r*-CPL, nearly mirror-imaged CD spectra were obtained according to the handedness of incident CPL. The

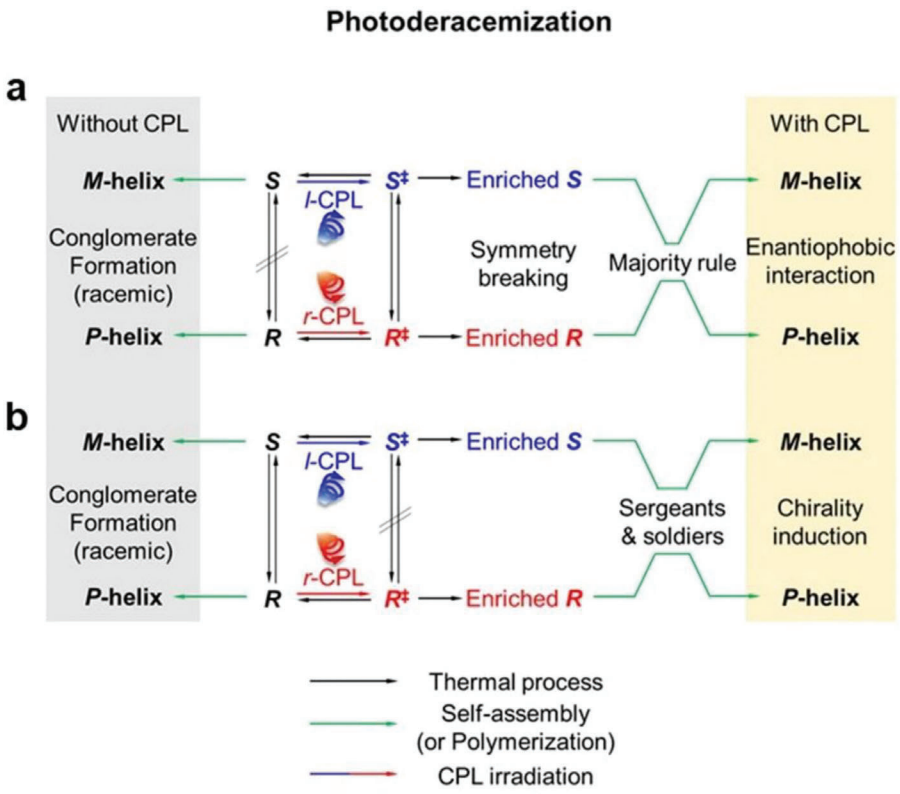

Scheme 3. Emergence of supramolecular chirality caused by the photoderacemization of a transiently chiral molecule upon CPL irradiation. Here, the interconversion processes are assumed to be adiabatic (i.e., direct interconversion without a common intermediate). a) Interconversion occurs in the excited state. The CPL-enriched conformer drives the homochiral self-assembly via enantiophobic interaction. The majority rule affords a dominant helical sense that matches the CPL handedness. b) Interconversion occurs in the ground state, but it is forbidden in the excited states. The CPL-enriched conformer as a chirality inducer interacts with another achiral molecules and aligns them in a helical order. A dominant helical sense is obtained following the sergeants-and-soldiers principle. While the mirror-imaged isomers produce the mirror-imaged helices such as *S*-enatiomer to *M*-helix and *R*-enatiomer to *P*-helix or vice versa, only one case was illustrated for clarity. It is also of note that the morphology of supramolecular chirality is not necessarily a helical structure. Here, *M*- and *P*-helixes are presented as a representative example.

ee determined based on the CD spectra was in the range of 0.4–1.6% depending on the cyclic structure and substituents.[69,70,72] Moreover, the photoresolved compounds were stable in absence of light.

Burnham and Schuster further investigated the propagation of CPL-induced chirality to a higher level using the bicyclic ketone derivative with a liquid crystalline pendent group as a chiroptical trigger in the LC transition (Figure 6c).[70] The chemical structure of the ketone was rendered to structurally resemble a liquid crystalline host molecule to ensure mixing and effective intermolecular interactions. The host molecules that were relatively transparent in the incident CPL wavelength were chosen as the "optical window" for the photoderacemization. The conversion of a nematic to cholesteric phase was observed by the CPL irradiation of the ketone–host mixture. Because the host molecules were aligned in a helical pattern in the cholesteric phase, the extent of chirality amplification in the bulk phase was estimated as the helical twisting power, which could be determined by measuring the helical pitch. Further, irradiation with unpolarized light reversed the transition, restoring the nematic phase. It should be also noted that Feringa and co-workers also demonstrated the propagation of chirality into a liquid crystalline mesophase using a photoresolvable helically shaped alkene.[73] Measuring the helical twisting power may be one way to quantify the ability of CPL in generating a chiral bias in supramolecular systems. However, this needs to be practiced carefully because one report indicates that irradiation of the liquid crystalline mixture with CPL in the presence of additional photoresolved dopant produced different helical pitches.[70]

Chiral amplification of the *ee* induced by the CPL-driven photoresolution into supramolecular chirality has been demonstrated in a polymeric system. Li et al. prepared a series of helical polyisocyanate copolymers comprising bicyclic ketone derivatives with achiral aliphatic side chains in the pendant.[71] Exposure of the polymer to CPL induced the partial photoderacemization of the ketone group. Interestingly, the minute *ee* afforded by CPL irradiation was transferred to the polyisocyanate backbone depending on the linkage (*o*-, *m*-, or *p*-) (Figure 6d). Furthermore, the CD spectra exhibited the CD activity corresponding to the handedness of the polyamide backbone, denoting that one helical sense was present in excess in the polymer chain because of the chirality transfer. The *m*- and *o*-copolymers afforded opposite backbone helicity for the same CPL, while the *p*-isomer was unable to induce the chirality transfer. This indicates that a subtle change in the chirophore–backbone interaction can cause remarkable differences in the supramolecular chirality. Further-

Table 2. Representative examples of supramolecular chirality via photoderacemization.

Chromophore	Features	Morphology	Absorption wavelength	Intensity	Ref.
Bicyclo[3,2,1]octan-3-one	– Aromatic and ester substituents – Axial chirality modulated by CPL	Cyclohexane solution	313 nm	1000 W[a)]	[69]
	– LC pendent group – Axial chirality modulated by CPL	MCH solution, LC droplet in glycol	313 nm		[70]
	– Main chain: polyisocyanate – Side chain: bicyclic ketone derivatives at *o*-, *m*-, and *p*-positions – Pendent group with axial chirality modulated by CPL	Cyclohexane solution	>305 nm		[71]
Thixanthene-ylidene and 12H-benzo[a]xanthene	– Sterically over crowded chiral alkene with axial chirality controlled by CPL – Reversible chiroptical molecular switch	*n*-Hexane and IPA solution, LC film	313 nm	200 W[b)]	[73]
Fluorene	– Main chain: polyfluorene – Reversibly controlled handedness by CPL – Deactivation chiral amplification process	Film	≈400 nm	50 mW cm^{-2}	[76]
		Film, suspension	≈400 nm	50 mW cm^{-2}	[74]
Triphenylamine	– Core: C_3-symmetry – Side chain: alkyl chain including diacetylene moiety – Radical cation produced by irradiation possible trigger stacking – Reversibly controlled handedness by CPL – Locking handedness by CPUL	DCE solution	365 nm	≈30 mW cm^{-2}	[81]
	– Core: C_3-symmetry – Stilbene-extended core – Side chain: alkyl chain including diacetylene moiety – Reversibly controlled handedness by CPL – Locking handedness by CPUL	Film	400 nm	≈30 mW cm^{-2}	[84]
Porphyrin	– Core: C_4-symmetry – Side chain: alkyl chain including diacetylene moiety – Reversibly controlled handedness by CPL – Locking handedness by UV	Organogel	398 nm	40 mW cm^{-2}	[82]

[a)] 200 W power of UV lamp with cutoff filter, focusing lens, linear polarizer and Fresnel rhomb [b)] 200 W power of mercury lamp with filter, polarizer and $\lambda/4$ plate.

more, the backbone handedness can be reversibly switched by alternating *l*- and *r*-CPL irradiation, and it can become racemic upon exposure to LPL. For the *m*-copolymer, the incorporation of only 2% of the ketone pendant, which generates less than 1% of *ee* upon CPL irradiation, could excessively twist the backbone in one direction and produce readily detectable CD intensity, despite 98% of the backbone containing achiral side chains. The chirality amplification can be understood based on the sergeants-and-soldiers principle: a few CPL-triggered ketone sergeants align the achiral soldiers to populate a specific helical conformation of the backbone, resulting in an amplified chiral response.

3.2. Polyfluorenes

Nakano reported that achiral polyfluorenes can adopt macromolecular helical conformation in their backbone via CPL irradiation.[75] Wang et al. investigated the optically activated fluorene-based polymers upon CPL irradiation in a reversible manner.[76] Moreover, they synthesized poly(di-*n*-octylfluorene-2,7-diyl) (PDOF), which is virtually racemic because the repeating unit lacking a stereocenter is connected via rotatable carbon–carbon bonds (**Figure 7**a). Nonetheless, optically active polyfluorene was induced upon CPL irradiation in the solid state with the reversible control of its handedness (Figure 7b). Moreover, they proposed that a preferentially handed helix is induced via photoderacemization, which involves a twisted-coplanar transition (TCT) of a transiently chiral fluorene diad. In another study, by examining a series of polyfluorene derivatives with the varying carbon number of the alkyl side chains, Wang et al. elaborated the diabetic mechanism by considering the deactivation of the coplanar intermediate state (Figure 7c,d).[74] They suggested that CPL transforms the conformation of the matching twist diad into coplanar via the enantiomer-selective photoexcitation, which decays back into *P*- and *M*-twists and eventually increasing the population of the CPL-mismatching twist. This causes the

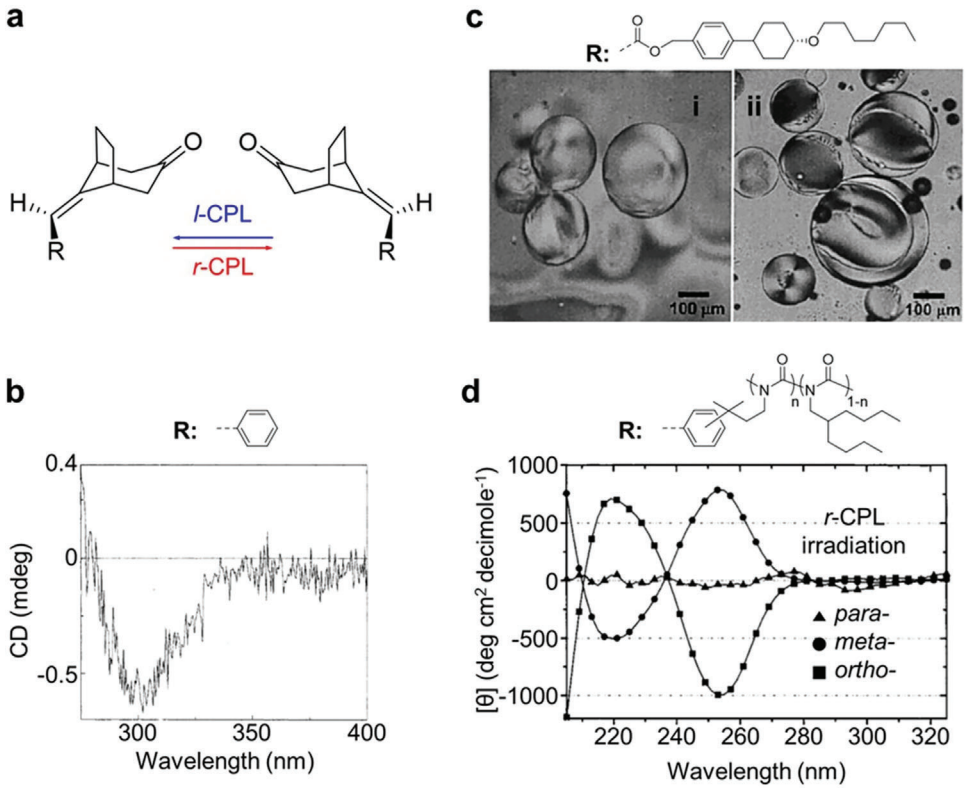

Figure 6. a) CPL-driven enantiomerization reaction of bicyclic ketone derivatives. Bicyclo[3,2,1]octan-3-one is given as an example. b) CD spectrum of the racemic phenyl-substituted bicyclic ketone in cyclohexane solution after CPL irradiation. Reproduced with permission.[69] Copyright 1995, American Chemical Society. c) Nematic-cholesteric transition of the ZLI1167 droplets containing a bicyclic ketone appended via a liquid crystalline motif. Optical microscopy images (i) before and (ii) after CPL irradiation. Reproduced with permission.[70] Copyright 1999, American Chemical Society. d) CD spectra of a polyisocyanate copolymer comprising 2-butylhexyl and bicyclic ketone side groups in *n*-hexane solution. The spectra were obtained after CPL irradiation in the n–π^* absorption region of ketone (≈300 nm). θ represents molar ellipticity. Connection of the ketone pendant to the backbone was via *p*- (triangles), *m*- (circles), and *o*-substitution (squares). The molar fraction (*n*) was 0.06, 0.02, and 0.02, respectively. Reproduced with permission.[71] Copyright 2000, American Chemical Society.

accumulation of the twist conformation with biased handedness. The *ee* was further amplified via propagation through the chain and also into the chains nearby, by biasing the deactivation equilibrium, termed "deactivation chirality amplification." Molecular weight of the polymer, side chain-driven interchain interaction, and packing structure were found to significantly affect the generation of the helical conformations and the wavelength or flux of incident light.

3.3. C_n-Symmetric Molecules

As well demonstrated, the self-assembly of small molecules into helical stacks is an effective way to transmit and amplify molecular chirality into the supramolecular level.[77] C_n-symmetric molecules comprising an aromatic-rich core and aliphatic side chains are typically used as monomeric building blocks in this "supramolecular polymerization." As in the case of polyisocyanates, the molecular chirality defined by a side-chain stereocenter determines the handedness of the supramolecular helical stack owing to the chirality transfer.[78] The majority rule and sergeants-and-soldiers principle also work for a racemic mixture and the co-assembly of a chiral sergeant with an achiral soldier, enabling chirality amplification at the supramolecular level.[79,80]

C_n-symmetric molecules are typically considered achiral if no stereocenters exist in the side chains. However, if a left- and right-tilted conformation of the core (commonly denoted as Λ and Δ, respectively) is thermodynamically more favored over the perfectly planar form and a rotational barrier is not negligible, then the molecule becomes transiently chiral. Thus, characterized by the relatively low rotational enantiomerization barrier, they are good building blocks for supramolecular polymerization with handedness control by CPL. To this end, designing a molecule to be photoresolvable by CPL is important. Because quantitative photoresolution is not possible, the CPL-enriched conformer should control the helicity during the self-assembly either by the majority-rule- or sergeants-and-soldiers-mediated processes.

Kim et al. reported the first example of CPL-driven supramolecular polymerization.[81] Their molecular design comprised a C_3-symmetric triphenylamine (TPA) core with diacetylene-containing side chains connected by an amide bond (DA-TPA) (**Figure 8**a–c). As is known, the TPA core possesses a propeller shape because of the sp^3 character of the central nitrogen atom.[83] Upon exposure to light in a chlorinated solvent, a TPA radical cation with a more planar conformation was formed

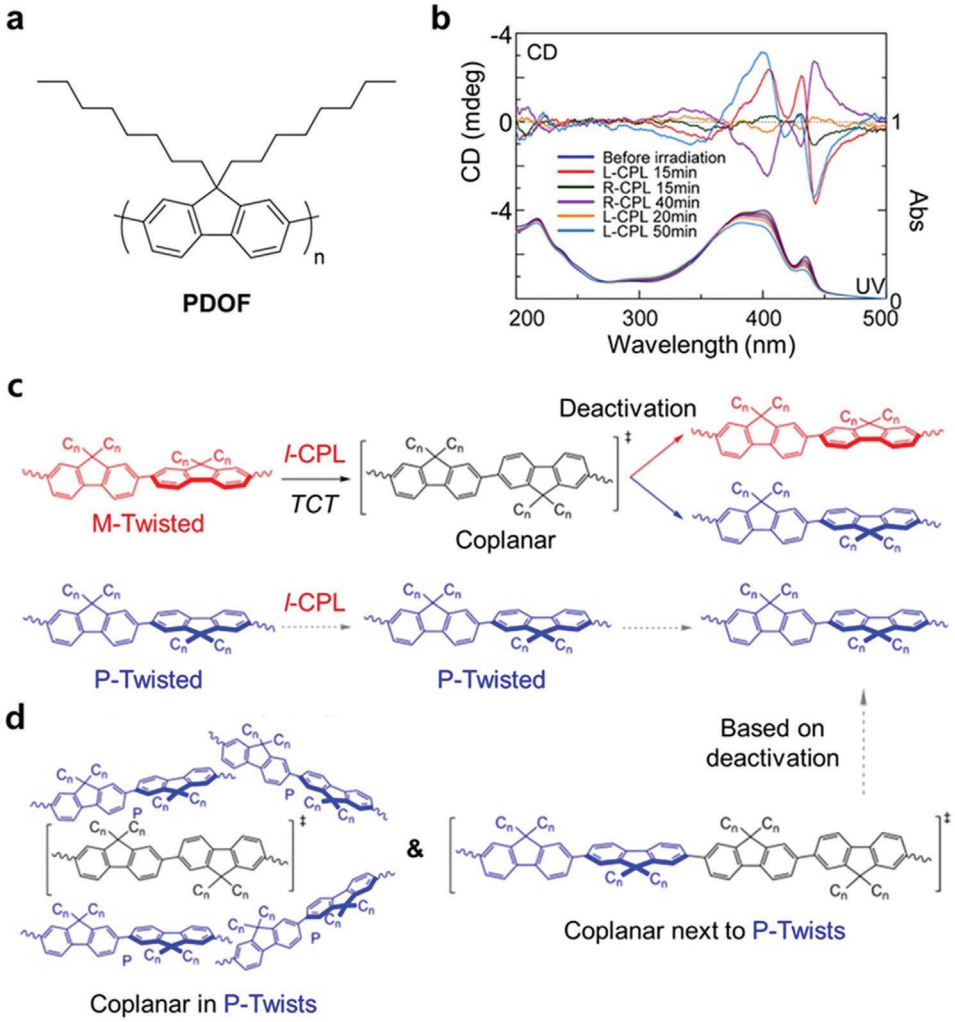

Figure 7. a) Molecular structure of PDOF. b) CD and UV spectra of PDOF upon CPL exposure. c) Enantiomer-selective photoderacemization of *M*-twisted fluorene diad comprising TCT and deactivation back to *M*- and *P*-diads. d) Deactivation-based chiral amplification through inter- (left) and intrachain (right) interactions. Reproduced with permission.[74] Copyright 2018, American Chemical Society.

by the photoinduced oxidation and triggered stacking presumably via electric dipole interaction. The self-assembled aggregates grown upon cooling exhibited strong CD intensity based on the rotational direction of the incident CPL. Reversible inversion of the CD sign with the opposite CPL and silent CD activity from unpolarized light supported the fact that the chiral information encoded in CPL was transmitted into the helical assembly. Utilizing the diacetylene motif for the topological polymerization discussed earlier, the assembly can be covalently fixed using UV irradiation. The reversal of the supramolecular helicity by CPL was locked by CPUL. Li et al. also reported the emergence of supramolecular chirality by CPL with a stilbene-extended TPA core.[84] While they interestingly demonstrated the induction, modulation, and locking of the supramolecular chirality by CPL, a plausible mechanism explaining the light–matter chirality transfer was not provided.

Similarly, Hu et al. reported the development of CPL-triggered asymmetric supramolecular assembly with a porphyrin-based molecule (Figure 8d,e).[82] A C_4-symmetric porphyrin derivative (TPPDA) containing a diacetylene moiety in its side chain was synthesized and self-assembled in chloroform upon UV irradiation. UV-induced protonation in the chlorinated medium was suggested to induce the distortion of the porphyrin core to a nonplanar structure. Furthermore, it was stated that the photoresolution would increase the population of the preferential enantiomeric protonated form matching the handedness of the incident CPL. Nanoaggregates with preferred helical chirality were produced in the initial stage, serving as a chiral template to amplify the chirality to the supramolecular level via the coassembly of the protonated and free base porphyrins. While the CPL-induced supramolecular chirality could be erased by heating and reproduced upon CPL exposure in a reversible manner, the photopolymerization of the peripheral diacetylene moiety in the solid state at 254 nm permanently locked the handedness of the assemblies and increased stability of the assembly.

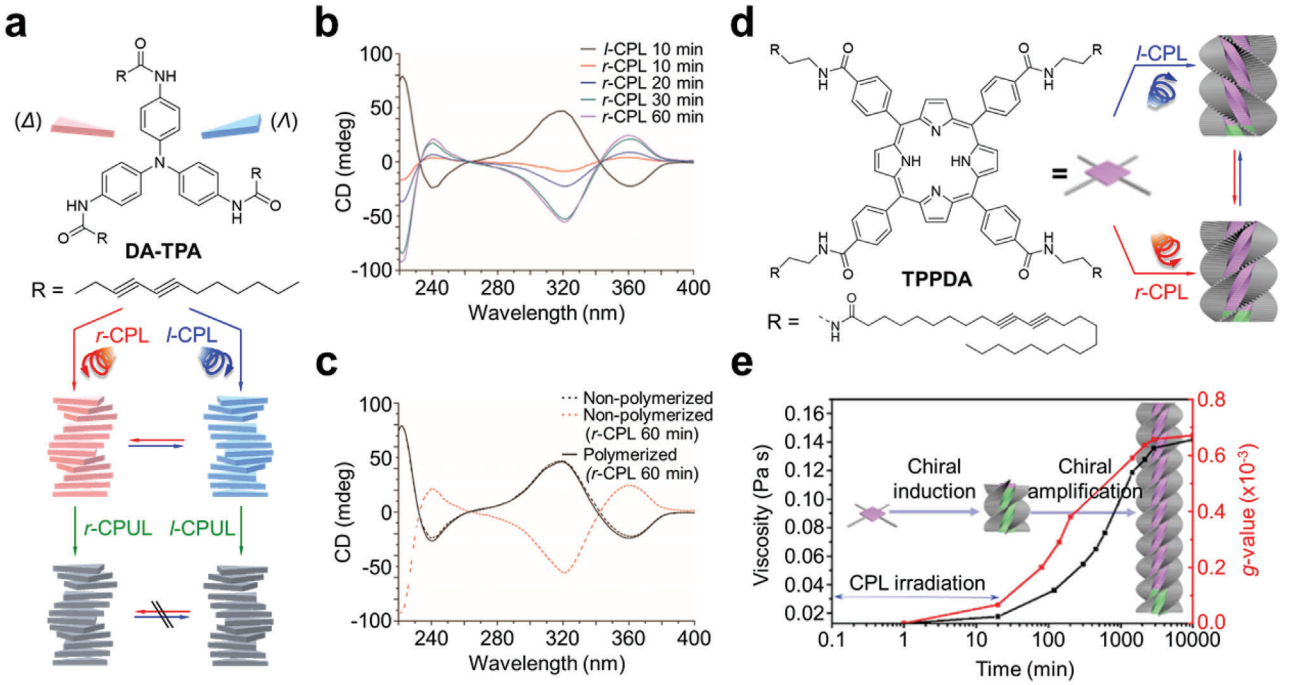

Figure 8. a–c) Light-induced self-assembly and locking process of the C_3-symmetric DA-TPA upon *l*- and *r*-CPL irradiation. a) Schematic illustration and b) emergence and inversion of the CD activity of DA-TPA in 1,2-dichloroethane solution upon CPL exposure. c) Effect of the photopolymerization of diacetylene moieties in DA-TPA by *l*-CPUL, which inhibits the inversion of CD activity by *r*-CPL. Reproduced with permission.[81] Copyright 2015, Springer Nature. Chirality induction and reversible switching of C_4-symmetric TPPDA by CPL: d) schematic presentation and e) time-resolved transition of viscosity and the anisotropic factor (*g*) upon CPL irradiation at 410 nm. Reproduced with permission.[82] Copyright 2019, The Royal Society of Chemistry.

4. Supramolecular Chirality via Asymmetric Photodestruction/Production

In the CPL-induced symmetry breaking, the asymmetric photodestruction/production process operates within the nanometer length scale, where each enantiomer reacts at different rates upon CPL irradiation.[66] Interconversion between the enantiomers is considered impossible (i.e., permanently chiral because of the high energy barrier for enantiomerization), and the photochemical reaction is assumed to be irreversible. Thus, an enantiomeric form is enriched after the asymmetric photodestruction reaction by preferentially consuming the opposite form. A relevant example is the asymmetric photolysis of amino acids upon CPL irradiation.[27] Photoproduction is also possible when an optically active product is produced as a result of the photochemical reaction. Similar to photoderacemization, the *ee* in the substrate and/or product state afforded by the asymmetric photodestruction/production can be amplified into the supramolecular level via self-assembly. The entire process is illustrated in **Scheme 4**. The representative examples of supramolecular chirality via asymmetric photodestruction/production are summarized in **Table 3**.

4.1. Asymmetric Photodestruction

Yeom et al. reported the transmission of chiral information in CPL to the handedness of self-assembling nanostructures comprising CdTe nanoparticles (NPs).[85] They prepared water-soluble NPs stabilized by achiral thioglycolic acid as a capping agent and illuminated them with *l*- and *r*-CPL (**Figure 9**). CPL exposure to the racemic NPs with truncated tetrahedron shape generated active NPs in an enantioselective manner based on the handedness of the incident CPL. Geometry-specific photooxidation of ligands occurred on the surface of a NP "enantiomer" with higher extinction coefficients. The asymmetric photodestruction afforded bare CdS NPs by replacing Te with S originating from the ligand, which has stronger propensity for self-assembly. A chiral nanoribbon comprising NPs with handedness matching that of CPL was produced due to the anisotropic interactions. The mirror-imaged CD spectra and electron microscopy images exhibiting opposite helical sense were obtained via *l*- and *r*-CPL irradiation. An *ee* as high as 30% was estimated from the microscopic analysis, which is more than ten times higher than that of the photoresolution of typical organic molecules. This may be particularly related to the fact that multiple photons are involved in the ligand photooxidation, which amplifies the differences between NPs.

4.2. Asymmetric Photoproduction

The chiroptical properties of nanostructures with noble metals have attracted significant interest owing to their unique plasmonic chirality.[86–89] As a representative example, Kotov and colleagues recently expanded the photon-to-matter chirality transfer principle to the assembly of gold NPs via the photoproduction process (**Figure 10**a–c).[87] To this end, they exposed CPL to the solution of Au(III) chloride hydrate and citrate. They identified

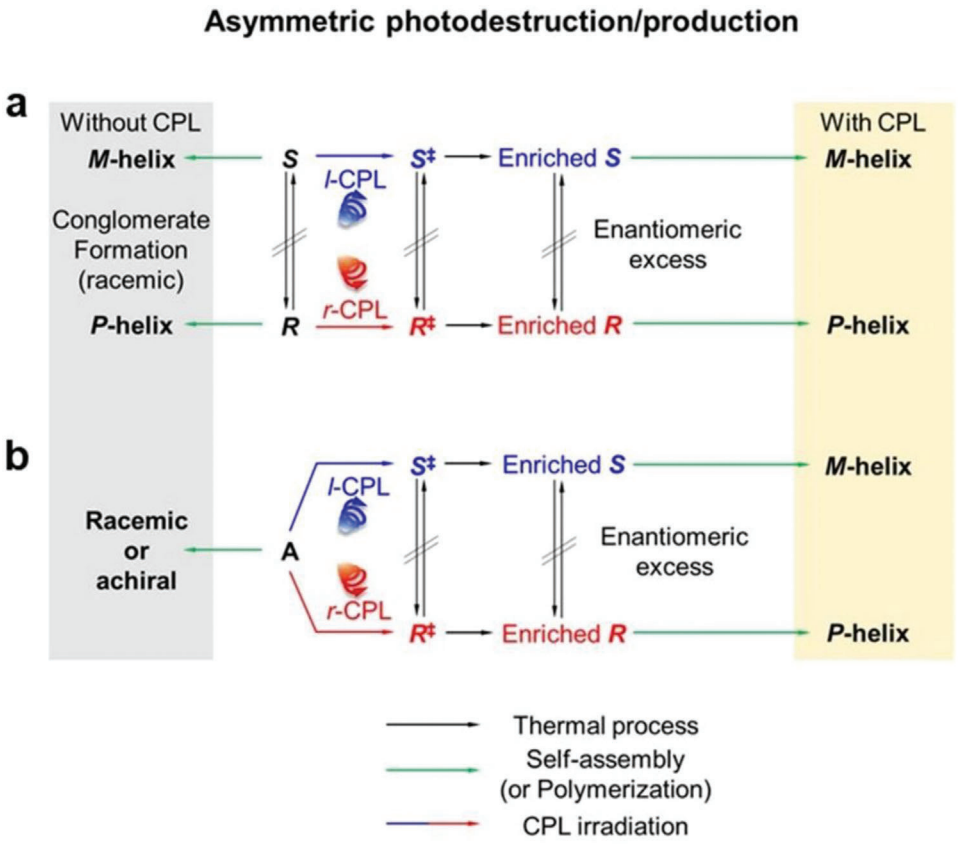

Scheme 4. Induction of the supramolecular chirality via asymmetric photodestruction and production processes upon CPL irradiation. The resulting *ee* propagates into the supramolecular level via self-assembly. a) Permanently chiral substrate where each isomer is consumed at different reaction rates by CPL. b) Achiral substrate affording optically active products at different rates by CPL. While the mirror-imaged isomers produce the mirror-imaged helices such as *S*-enantiomer to *M*-helix and *R*-enantiomer to *P*-helix or vice versa, only one case was illustrated for clarity. It is also of note that the morphology of supramolecular chirality is not necessarily a helical structure. Here, *M*- and *P*-helixes are presented as a representative example.

Table 3. Representative examples of supramolecular chirality via asymmetric photodestruction/production.

Chromophore	Features	Morphology	Absorption wavelength	Intensity	Ref.
CdTe	– Activation: site-selective photodestruction of TGA-ligand by CPL				
– Self-assembly into nanoribbons from chiral CdS NPs	NP assembly	543 nm	0.03, 0.061 mW		[85]
Au	– Directions of induced plasmonic forces decided by incident CPL				
– Self-assembly depending on the directions of plasmonic forces	NP	543 nm	100 mW cm^{-2}		[87]
Au and Pb	– Localized electric field distributions driven by CPL				
– Chiral deposition of PbO_2 by PICS	Nanocuboid on a substrate	>520 nm	≈17 mW cm^{-2}		[87]
	– Localized electric field distributions driven by CPL				
– Chiral deposition of PbO_2 by PICS					
– Reversible pathway by UV irradiation			≈19 mW cm^{-2}		[87]
Allyl-(4-mercapto-1-oxobutan-2-yl)carbamate	– Asymmetric thiol–ene polymerization				
– CPL-driven enrichment of one radical enantiomer	Acetonitrile solution	313 nm	20 mW cm^{-2}		[90]

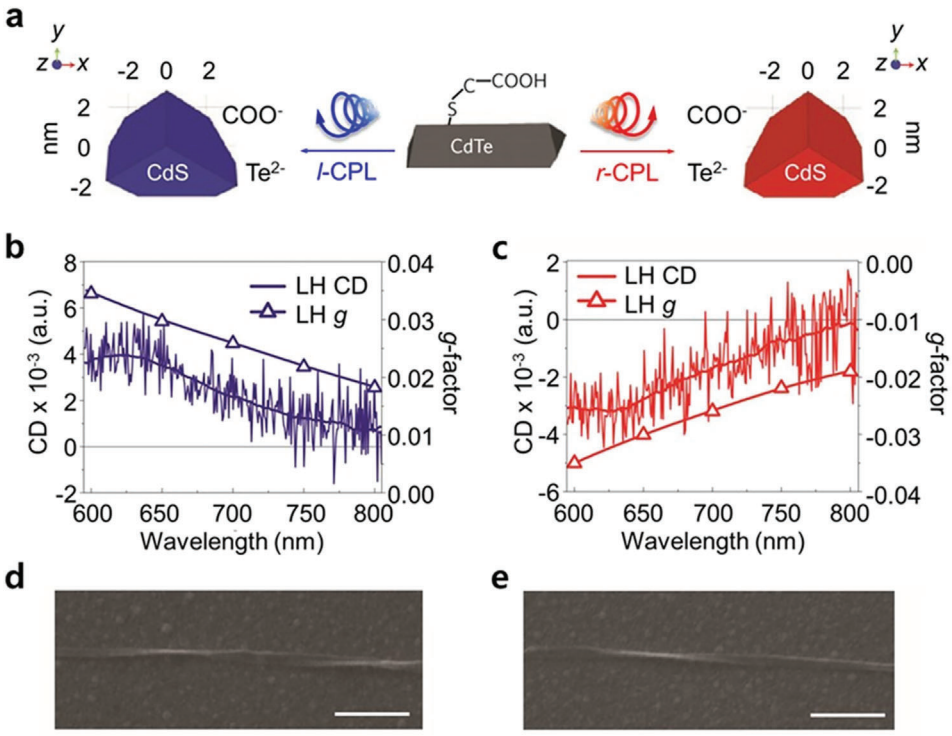

Figure 9. a) Schematic representation of the transition from CdTe to chiral CdS clusters by CPL irradiation. CD spectra and the calculated anisotropic factor, *g*, of a single nanoribbon with b) left-handedness (LH) and c) right-handedness (RH) irradiated by *l*- and *r*-CPL, respectively. SEM images of the nanoribbon with d) left-handedness and e) right-handedness. Scale bars indicate 500 nm. Reproduced with permission.[85] Copyright 2014, Springer Nature.

two steps for the formation of chiral Au nanostructures: partial photoreduction of Au(III) ions to produce clusters and the growth of the clusters wherein the photoinduced plasmonic forces twist the geometry of growing clusters in the out-of-plane direction according to the handedness of the incident light. Subsequently, chiral Au nanostructures with opposite CD signs were produced after irradiation of *l*- and *r*-CPL, despite their irregular shape.

Saito and Tatsuma reported the fabrication of chiral plasmonic nanostructures using the asymmetric electric field distributions from incident CPL for site-specific electrochemical deposition (Figure 10d–f).[88] Au nanocuboids on a TiO_2 substrate were immersed in a solution containing Pb(II) ions and were then exposed to CPL. Subsequently, localized and twisted electric fields were generated upon CPL irradiation at specific corners depending on the handedness of light. Plasmon-induced charge transfer (PICS) between Au nanocuboid and TiO_2 caused by the electric field allowed the oxidation of PdO_2 at the designated corners with 43% of *ee*. Moreover, strong CD responses were observed after CPL exposure. Additionally, chirality could be reversibly switched by reducing the deposited PbO_2 with nonpolarized UV light and then irradiating with CPL.[89]

In organic systems, Hu et al. reported CPL-induced enantioselective thiol–ene polymerization.[90] They synthesized a racemic AB-type monomer comprising thiol and vinyl moieties that can react with each other under light irradiation (**Figure 11**). Upon irradiation, symmetry breaking occurred due to the molar circular dichroism of the monomers for *l*- and *r*-CPL, subsequently affording one preferential thiyl radical enantiomer. The addition of the thiyl radical onto a vinyl bond in a step-growth manner formed chiral polymers with noticeable optical activities. The same principle can be applied to thiol–yne polymerization, which yields chiral hyperbranched polymers. The asymmetric photoproduction mechanism is supported by the kinetics study, which exhibits that CPL irradiation enhances the reaction rate of a chirality-matching monomer and suppresses the stereoisomer. Based on the specific rotation of the monomer, *ee* of more than 15% was estimated in the produced polymer. Furthermore, longer irradiation decreased the optical activity, eventually tending close to zero. Thus, the participation of a less reactive stereoisomer in the late stage of polymerization causes a compositional drift.

5. Summary and Outlook

In this review, we present the mechanisms of the supramolecular chirality driven by CPL as chiral physical force. The preferential interaction between CPL and one enantiomer can induce and modulate the chirality at the supramolecular level. In particular, this review has focused on the possible mechanisms for the amplification process of the chiral bias from photochromic building blocks to supramolecular chiral structures upon CPL irradiation: stereoregular packing/polymerization, photoderacemization, and asymmetric photodestruction/production. As repre-

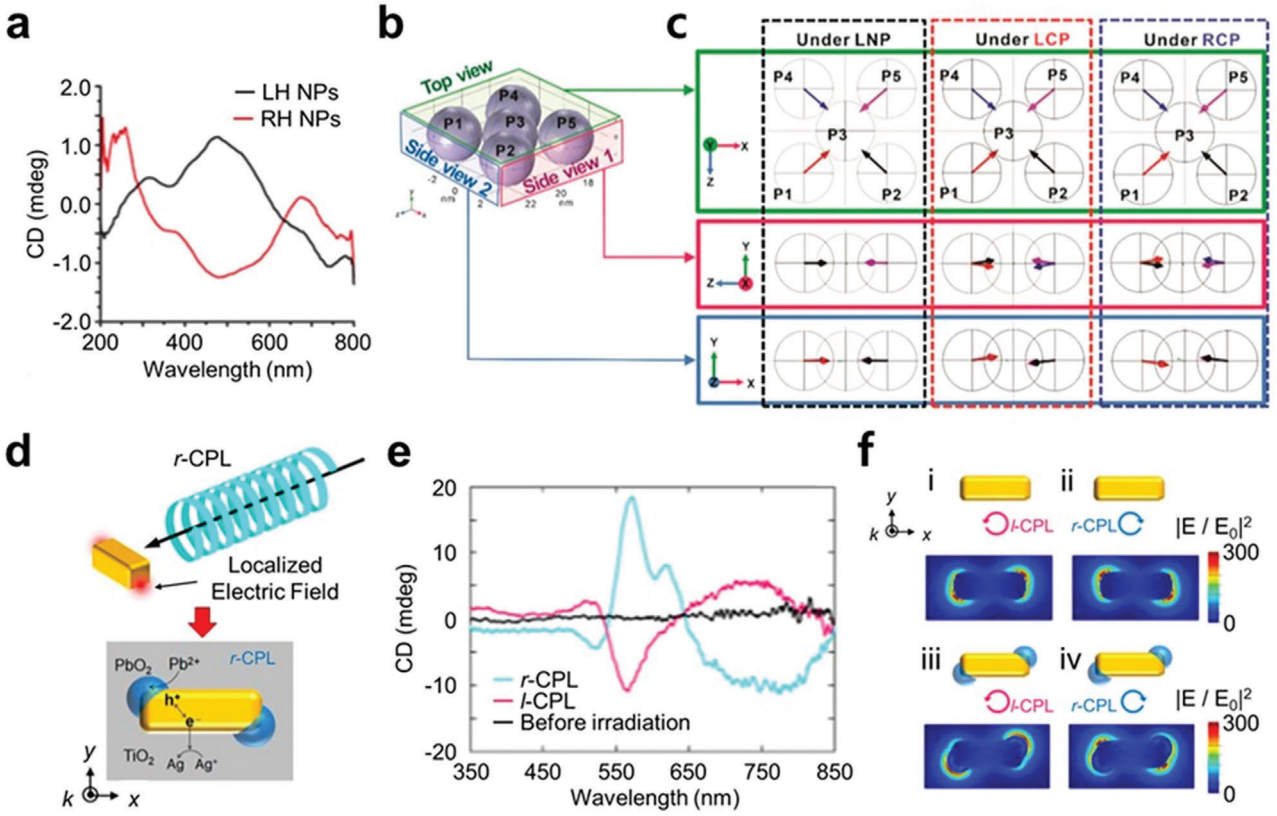

Figure 10. a–c) CPL-driven formation of chiral Au nanostructures. a) CD spectra of Au NPs obtained after 50 min of CPL irradiation. b) Model for closely packed Au NP assemblies from P1 to P5. c) Volume arrow plot for the plasmonic forces on each Au NPs (P1, red; P2, black; P3, green; P4, blue; and P5, magenta) under LPL irradiation and left- and right-handed CPL. d–f) Site-specific PtO_2 deposition onto Au nanocuboid via CPL. Reproduced with permission.[87] Copyright 2019, American Chemical Society. d) Schematic of the chiral nanostructure formation involving PICS. e) CD spectra of the obtained PtO_2-deposited Au nanocuboids after *l*- (purple) and *r*-CPL (cyan) irradiation. f) Electric field distributions around Au nanocuboid before (i and ii) and after CPL irradiation (iii and iv). Reproduced with permission.[88] Copyright 2018, American Chemical Society.

sentative examples, azobenzene derivatives, polydiacetylene, bicyclic ketone, polyfluorenes, C_n-symmetric molecules, and inorganic nanomaterials have been summarized.

Some basic rules for designing supramolecular systems highly responsible to CPL can be deduced as follows. 1) High *g* factor is essential for efficient symmetry breaking by CPL. Generally, the building block should exhibit high molecular dichroism for the target wavelength while the extinction coefficient is small to maximize the *g* factor. 2) The photoreaction quantum yield should be high. The system should be also transparent to the target wavelength to avoid loss of photons by undesirable absorption. The chemical structure of the building block should be carefully designed and also the medium (i.e., solvent) should be carefully chosen. 3) The broken symmetry should effectively propagate into the supramolecular level via strong enantiophobic interaction with homochiral preference. Heterochiral propagation should be inhibited. This can be related to the high helix reversal penalty in the helical conformation. Collective expression of the chiral bias in the building block as a result of the multiphoton-involved photochemical reaction may amplify the asymmetry as in the case of nanoparticles. 4) To maximize the CD activity as a representative chiroptical response, high rotatory strength should be attained in the supramolecular level. Computation-aided design of the molecular structure will be helpful. Inorganic nanomaterials and organic–inorganic hybrids are expected to be more actively sought as potential building blocks with superior optical properties.

The CPL-induced supramolecular chirality can be potentially applied to chiral sensing system. Specifically, the photoresponsive properties of dimer LCs with azo unit can produce a well-aligned racemic chiral photonic film under UV irradiation due to *trans–cis* isomerization.[96] By using the racemic photonic film with supramolecular chiral domains, the optical activity of the chiral substances can be readily discriminated visually as each chiral domain reflects a CPL corresponding to a given handedness. Furthermore, the tunable supramolecular chirality using CPL irradiation promises to lead circularly polarized luminescence with stimuli-responsive chiroptical properties, which can be applied to 3D displays, optical data storage, and photoelectric devices.[97]

Finally, we anticipate that this review aid understanding of the detailed mechanisms for the supramolecular chirality process induced by a chiral bias upon CPL irradiation, thus proving the origins and evolution of living organisms and nature as well as expanding to developing applications such as chiral recognition and switching, electro-optics, and biological fields.[98–101]

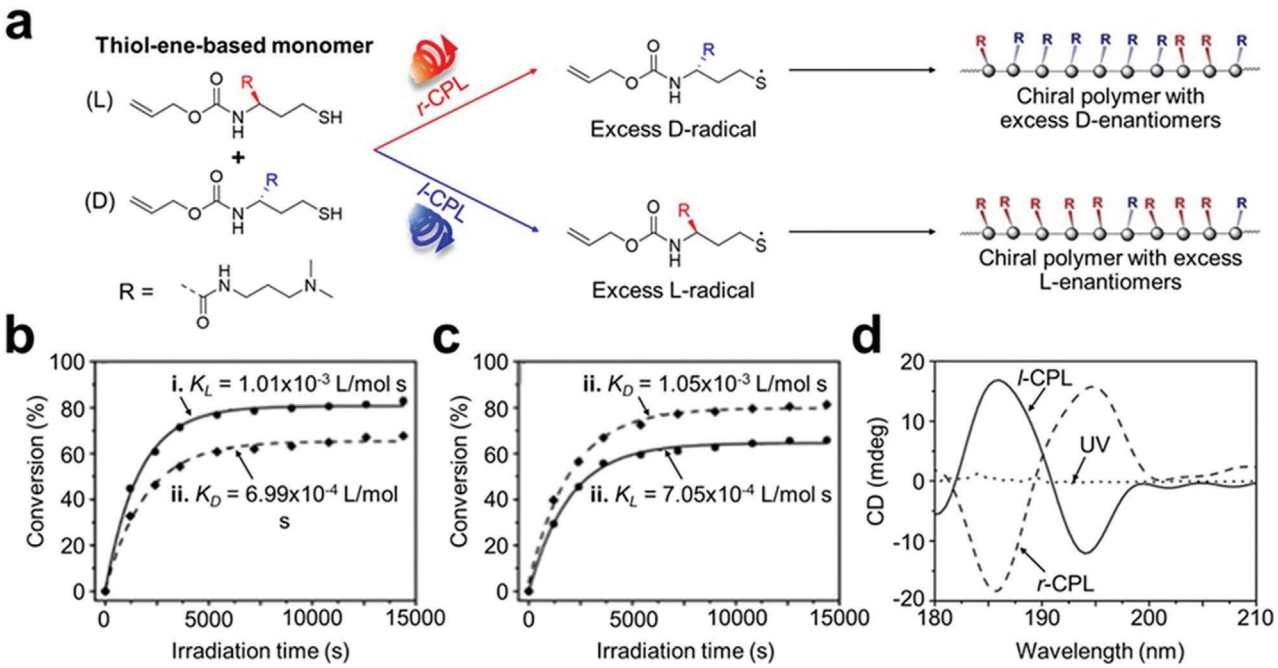

Figure 11. a) Schematic representation of the formation of optically active polymer chains from racemic monomers through CPL-driven enantioselective thiol–ene polymerization. Conversion of (i) L- and (ii) D-monomers as a function of b) *l*- and c) *r*-CPL irradiation time. d) CD spectra of hyperbranched polymers obtained via asymmetric thiol–yne polymerization using *l*-CPL (solid line), *r*-CPL (dashed line), and unpolarized UV light (dotted line). Reproduced with permission.[90] Copyright 2017, The Royal Society of Chemistry.

Acknowledgements

J.S.K. and N.K. contributed equally to this work. This work was supported by the National Research Foundation of Korea (NRF-2018R1A5A1025208).

Conflict of Interest

The authors declare no conflict of interest.

Keywords

circularly polarized light, chirality transfer, supramolecular chirality, symmetry breaking

Received: September 28, 2021
Revised: October 22, 2021
Published online:

[1] J. Bailey, A. Chrysostomou, J. H. Hough, T. M. Gledhill, A. Mccall, S. Clark, F. Ménard, M. Tamura, *Science* **1998**, *281*, 672.
[2] N. Globus, R. D. Blandford, *Astrophys. J.* **2020**, *895*, L11.
[3] S. Vandenbussche, J. Reisse, K. Bartik, J. Lievin, *Chirality* **2011**, *23*, 367.
[4] K. Soai, T. Kawasaki, A. Matsumoto, *Acc. Chem. Res.* **2014**, *47*, 3643.
[5] Y. Wang, J. Chou, Y. Sun, S. Wen, S. Vasilescu, H. Zhang, *Mater. Sci. Eng., C* **2019**, *101*, 650.
[6] W. L. Noorduin, A. A. C. Bode, M. Van Der Meijden, H. Meekes, A. F. Van Etteger, W. J. P. Van Enckevort, P. C. M. Christianen, B. Kaptein, R. M. Kellogg, T. Rasing, E. Vlieg, *Nat. Chem.* **2009**, *1*, 729.
[7] M. M. Green, N. C. Peterson, T. Sato, A. Teramoto, R. Cook, S. Lifson, *Science* **1995**, *268*, 1860.
[8] Y. Zhang, B. Xia, Y. Hu, Q. Zhu, X. Lin, Q. Wu, *ACS Macro Lett.* **2019**, *8*, 1188.
[9] R. Schreiber, N. Luong, Z. Fan, A. Kuzyk, P. C. Nickels, T. Zhang, D. M. Smith, B. Yurke, W. Kuang, A. O. Govorov, T. Liedl, *Nat. Commun.* **2013**, *4*, 2948.
[10] P. Duan, Y. Li, L. Li, J. Deng, M. Liu, *J. Phys. Chem. B* **2011**, *115*, 3322.
[11] Y. Li, T. Wang, M. Liu, *Soft Matter* **2007**, *3*, 1312.
[12] Y. Cai, Z. Guo, J. Chen, W. Li, L. Zhong, Y. Gao, L. Jiang, L. Chi, H. Tian, W.-H. Zhu, *J. Am. Chem. Soc.* **2016**, *138*, 2219.
[13] G. Liu, J. Sheng, W. L. Teo, G. Yang, H. Wu, Y. Li, Y. Zhao, *J. Am. Chem. Soc.* **2018**, *140*, 16275.
[14] D. Niu, Y. Jiang, L. Ji, G. Ouyang, M. Liu, *Angew. Chem., Int. Ed.* **2019**, *58*, 5946.
[15] F. Wang, M. Qin, T. Peng, X. Tang, A. Yinme Dang-I, C. Feng, *Langmuir* **2018**, *34*, 7869.
[16] L. Zhang, H.-X. Wang, S. Li, M. Liu, *Chem. Soc. Rev.* **2020**, *49*, 9095.
[17] N. Shukla, M. A. Bartel, A. J. Gellman, *J. Am. Chem. Soc.* **2010**, *132*, 8575.
[18] J. Ding, M. Zhang, H. Dai, C. Lin, *Chirality* **2018**, *30*, 1245.
[19] B. Zhu, F. Zhao, J. Yu, Z. Wang, Y. Song, Q. Li, *New J. Chem.* **2018**, *42*, 13421.
[20] R. Bruno, N. Marino, L. Bartella, L. Di Donna, G. De Munno, E. Pardo, D. Armentano, *Chem. Commun.* **2018**, *54*, 6356.
[21] K. Tamura, T. Miyabe, H. Iida, E. Yashima, *Polym. Chem.* **2011**, *2*, 91.
[22] H. Wang, X. Yong, H. Huang, H. Yu, Y. Wu, J. Deng, *Polym. Chem.* **2019**, *10*, 1780.
[23] J. Liu, F. Yuan, X. Ma, D.-I. Y. Auphedeous, C. Zhao, C. Liu, C. Shen, C. Feng, *Angew. Chem., Int. Ed.* **2018**, *57*, 6475.
[24] B. Mao, M. Fañanás-Mastral, B. L. Feringa, *Chem. Rev.* **2017**, *117*, 10502.

[25] Q. Jin, L. Zhang, H. Cao, T. Wang, X. Zhu, J. Jiang, M. Liu, *Langmuir* **2011**, *27*, 13847.
[26] M. Raynal, F. Portier, P. W. N. M. Van Leeuwen, L. Bouteiller, *J. Am. Chem. Soc.* **2013**, *135*, 17687.
[27] C. Meinert, S. V. Hoffmann, P. Cassam-Chenaï, A. C. Evans, C. Giri, L. Nahon, U. J. Meierhenrich, *Angew. Chem., Int. Ed.* **2014**, *53*, 210.
[28] P. K. Hashim, N. Tamaoki, *ChemPhotoChem* **2019**, *3*, 347.
[29] S. Panja, D. J. Adams, *Chem. Soc. Rev.* **2021**, *50*, 5165.
[30] L. Li, R. Sun, R. Zheng, Y. Huang, *Mater. Des.* **2021**, *205*, 109759.
[31] Y.-H. Lee, L. He, Y.-T. Chan, *Macromol. Rapid Commun.* **2018**, *39*, 1800465.
[32] X. Yan, F. Wang, B. Zheng, F. Huang, *Chem. Soc. Rev.* **2012**, *41*, 6042.
[33] J.-M. Lehn, *Proc. Natl. Acad. Sci. USA* **2002**, *99*, 4763.
[34] B. L. Feringa, R. A. Van Delden, *Angew. Chem., Int. Ed.* **1999**, *38*, 3418.
[35] S.-W. Choi, S. Kawauchi, N. Y. Ha, H. Takezoe, *Phys. Chem. Chem. Phys.* **2007**, *9*, 3671.
[36] Y. Okawa, M. Akai-Kasaya, Y. Kuwahara, S. K. Mandal, M. Aono, *Nanoscale* **2012**, *4*, 3013.
[37] X. Cheng, T. Miao, Y. Qian, Z. Zhang, W. Zhang, X. Zhu, *Int. J. Mol. Sci.* **2020**, *21*, 6186.
[38] G. Iftime, F. L. Labarthet, A. Natansohn, P. Rochon, *J. Am. Chem. Soc.* **2000**, *122*, 12646.
[39] M.-J. Kim, B.-G. Shin, J.-J. Kim, D.-Y. Kim, *J. Am. Chem. Soc.* **2002**, *124*, 3504.
[40] L. Wang, L. Yin, W. Zhang, X. Zhu, M. Fujiki, *J. Am. Chem. Soc.* **2017**, *139*, 13218.
[41] B. L. Feringa, R. A. Van Delden, N. Koumura, E. M. Geertsema, *Chem. Rev.* **2000**, *100*, 1789.
[42] H. M. D. Bandara, S. C. Burdette, *Chem. Soc. Rev.* **2012**, *41*, 1809.
[43] A. A. Beharry, O. Sadovski, G. A. Woolley, *J. Am. Chem. Soc.* **2011**, *133*, 19684.
[44] S. Sun, S. Liang, W.-C. Xu, G. Xu, S. Wu, *Polym. Chem.* **2019**, *10*, 4389.
[45] Y. Li, Y. He, X. Tong, X. Wang, *J. Am. Chem. Soc.* **2005**, *127*, 2402.
[46] W. Wang, C. Du, X. Wang, X. He, J. Lin, L. Li, S. Lin, *Angew. Chem., Int. Ed.* **2014**, *53*, 12116.
[47] L. Nikolova, T. Todorov, M. Ivanov, F. Andruzzi, S. Hvilsted, P. S. Ramanujam, *Opt. Mater.* **1997**, *8*, 255.
[48] L. Nikolova, L. Nedelchev, T. Todorov, T. Petrova, N. Tomova, V. Dragostinova, P. S. Ramanujam, S. Hvilsted, *Appl. Phys. Lett.* **2000**, *77*, 657.
[49] M. Alaasar, S. Poppe, Q. Dong, F. Liu, C. Tschierske, *Angew. Chem., Int. Ed.* **2017**, *56*, 10801.
[50] J. Royes, L. Oriol, R. M. Tejedor, M. Piñol, *Polymers* **2019**, *11*, 885.
[51] T. Miao, L. Yin, X. Cheng, Y. Zhao, W. Hou, W. Zhang, X. Zhu, *Polymers* **2018**, *10*, 612.
[52] M. Otaki, R. Kumai, H. Sagayama, H. Goto, *Macromolecules* **2019**, *52*, 2340.
[53] S.-W. Choi, T. Izumi, Y. Hoshino, Y. Takanishi, K. Ishikawa, J. Watanabe, H. Takezoe, *Angew. Chem., Int. Ed.* **2006**, *45*, 1382.
[54] S.-W. Choi, T. Fukuda, Y. Takanishi, K. Ishikawa, H. Takezoe, *Jpn. J. Appl. Phys.* **2006**, *45*, 447.
[55] S.-W. Choi, N. Y. Ha, K. Shiromo, N. V. S. Rao, M. Kr Paul, T. Toyooka, S. Nishimura, J. W. Wu, B. Park, Y. Takanishi, K. Ishikawa, H. Takezoe, *Phys. Rev. E* **2006**, *73*, 021702.
[56] H. Takezoe, Y. Takanishi, *Jpn. J. Appl. Phys.* **2006**, *45*, 597.
[57] G. Yang, S. Zhang, J. Hu, M. Fujiki, G. Zou, *Symmetry* **2019**, *11*, 474.
[58] G. Zou, H. Jiang, Q. Zhang, H. Kohn, T. Manaka, M. Iwamoto, *J. Mater. Chem.* **2010**, *20*, 285.
[59] Y. Xu, H. Jiang, Q. Zhang, F. Wang, G. Zou, *Chem. Commun.* **2014**, *50*, 365.
[60] G. Yang, L. Han, H. Jiang, G. Zou, Q. Zhang, D. Zhang, P. Wang, H. Ming, *Chem. Commun.* **2014**, *50*, 2338.
[61] D. Takajo, K. Sudoh, *Langmuir* **2019**, *35*, 2123.
[62] T. Manaka, H. Kon, Y. Ohshima, G. Zou, M. Iwamoto, *Chem. Lett.* **2006**, *35*, 1028.
[63] G. Zou, H. Jiang, H. Kohn, T. Manaka, M. Iwamoto, *Chem. Commun.* **2009**, 5627.
[64] C. He, G. Yang, Y. Kuai, S. Shan, L. Yang, J. Hu, D. Zhang, Q. Zhang, G. Zou, *Nat. Commun.* **2018**, *9*, 5117.
[65] Y. Xu, G. Yang, H. Xia, G. Zou, Q. Zhang, J. Gao, *Nat. Commun.* **2014**, *5*, 5050.
[66] Y. Inoue, *Chem. Rev.* **1992**, *92*, 741.
[67] C. Tschierske, G. Ungar, *ChemPhysChem* **2016**, *17*, 9.
[68] S. M. Morrow, A. J. Bissette, S. P. Fletcher, *Nat. Nanotechnol.* **2017**, *12*, 410.
[69] Y. Zhang, G. B. Schuster, *J. Org. Chem.* **1995**, *60*, 7192.
[70] K. S. Burnham, G. B. Schuster, *J. Am. Chem. Soc.* **1999**, *121*, 10245.
[71] J. Li, G. B. Schuster, K.-S. Cheon, M. M. Green, J. V. Selinger, *J. Am. Chem. Soc.* **2000**, *122*, 2603.
[72] M. Suarez, G. B. Schuster, *J. Am. Chem. Soc.* **1995**, *117*, 6732.
[73] N. P. M. Huck, W. F. Jager, B. De Lange, B. L. Feringa, *Science* **1996**, *273*, 1686.
[74] Y. Wang, T. Harada, L. Q. Phuong, Y. Kanemitsu, T. Nakano, *Macromolecules* **2018**, *51*, 6865.
[75] T. Nakano, *Chem. Rec.* **2014**, *14*, 369.
[76] Y. Wang, T. Sakamoto, T. Nakano, *Chem. Commun.* **2012**, *48*, 1871.
[77] M. Liu, L. Zhang, T. Wang, *Chem. Rev.* **2015**, *115*, 7304.
[78] Y. Dorca, E. E. Greciano, J. S. Valera, R. Gómez, L. Sánchez, *Chem. - Eur. J.* **2019**, *25*, 5848.
[79] M. M. J. Smulders, P. J. M. Stals, T. Mes, T. F. E. Paffen, A. P. H. J. Schenning, A. R. A. Palmans, E. W. Meijer, *J. Am. Chem. Soc.* **2010**, *132*, 620.
[80] M. M. J. Smulders, A. P. H. J. Schenning, E. W. Meijer, *J. Am. Chem. Soc.* **2008**, *130*, 606.
[81] J. Kim, J. Lee, W. Y. Kim, H. Kim, S. Lee, H. C. Lee, Y. S. Lee, M. Seo, S. Y. Kim, *Nat. Commun.* **2015**, *6*, 6959.
[82] J. Hu, Y. Xie, H. Zhang, C. He, Q. Zhang, G. Zou, *Chem. Commun.* **2019**, *55*, 4953.
[83] C. B. Duke, J. W.-P. Lin, A. Paton, W. R. Salaneck, K. L. Yip, *Chem. Phys. Lett.* **1979**, *61*, 402.
[84] C. Park, J. Lee, T. Kim, J. Lim, J. Park, W. Y. Kim, S. Y. Kim, *Molecules* **2020**, *25*, 402.
[85] J. Yeom, B. Yeom, H. Chan, K. W. Smith, S. Dominguez-Medina, J. H. Bahng, G. Zhao, W.-S. Chang, S.-J. Chang, A. Chuvilin, D. Melnikau, A. L. Rogach, P. Zhang, S. Link, P. Král, N. A. Kotov, *Nat. Mater.* **2015**, *14*, 66.
[86] S. Wang, Y. Zhang, X. Qin, L. Zhang, Z. Zhang, W. Lu, M. Liu, *ACS Nano* **2020**, *14*, 6087.
[87] J.-Y. Kim, J. Yeom, G. Zhao, H. Calcaterra, J. Munn, P. Zhang, N. Kotov, *J. Am. Chem. Soc.* **2019**, *141*, 11739.
[88] K. Saito, T. Tatsuma, *Nano Lett.* **2018**, *18*, 3209.
[89] K. Morisawa, T. Ishida, T. Tatsuma, *ACS Nano* **2020**, *14*, 3603.
[90] G. Yang, Y. Y. Xu, Z. D. Zhang, L. H. Wang, X. H. He, Q. J. Zhang, C. Y. Hong, G. Zou, *Chem. Commun.* **2017**, *53*, 1735.
[91] D. Hore, Y. Wu, A. Natansohn, P. Rochon, *J. Appl. Phys.* **2003**, *94*, 2162.
[92] Y. Wu, A. Natansohn, P. Rochon, *Macromolecules* **2004**, *37*, 6801.
[93] R. M. Tejedor, L. Oriol, J. L. Serrano, F. P. Ureña, J. J. L. González, *Adv. Funct. Mater.* **2007**, *17*, 3486.
[94] J. Barberá, L. Giorgini, F. Paris, E. Salatelli, R. M. Tejedor, L. Angiolini, *Chem. - Eur. J.* **2008**, *14*, 11209.
[95] G. Zou, Y. Wang, Q. Zhang, H. Kohn, T. Manaka, M. Iwamoto, *Polymer* **2010**, *51*, 2229.
[96] W. Park, J. M. Wolska, D. Pociecha, E. Gorecka, D. K. Yoon, *Adv. Opt. Mater.* **2019**, *7*, 1901399.

[97] X. Tang, D. Chu, H. Jiang, W. Gong, C. Jiang, Y. Cui, Y. Liu, *Mater. Chem. Front.* **2020**, *4*, 2772.
[98] J. Hu, T. Zhu, C. He, Y. Zhang, Q. Zhang, G. Zou, *J. Mater. Chem. C* **2017**, *5*, 5135.
[99] E. E. Greciano, R. Rodríguez, K. Maeda, L. Sánchez, *Chem. Commun.* **2020**, *56*, 2244.
[100] A. B. Kanj, J. Bürck, N. Vankova, C. Li, D. Mutruc, A. Chandresh, S. Hecht, T. Heine, L. Heinke, *J. Am. Chem. Soc.* **2021**, *143*, 7059.
[101] C. Kulkarni, R. H. N. Curvers, G. Vantomme, D. J. Broer, A. R. A. Palmans, S. C. J. Meskers, E. W. Meijer, *Adv. Mater.* **2021**, *33*, 2005720.

Jun Su Kang is currently a Ph.D. candidate in Prof. Myungeun Seo's group in the Department of Chemistry at Korea Advanced Institute of Science and Technology (KAIST). He received his B.S. from the Department of Chemistry at Yonsei University, Republic of Korea, in 2018. His research interest is related to supramolecular chiral materials.

Namhee Kim is currently an M.S./Ph.D. student under the guidance of Prof. Byeong-Su Kim in the Department of Chemistry at Yonsei University. She received her B.S. from the Department of Chemistry at Chungnam National University, Republic of Korea, in 2020. Her research interests include nanomaterials and polymers for energy conversion.

Taehyung Kim is currently a Ph.D. student under the guidance of Prof. Byeong-Su Kim in the Department of Energy Engineering at the Ulsan National Institute of Science and Technology (UNIST). In 2017, he received his B.S. from the Department of Energy Engineering at UNIST. His research interests include the design and synthesis of redox-active covalent organic frameworks for lithium-ion batteries.

Myungeun Seo is a polymer chemist interested in controlled synthesis of polymeric and supramolecular materials and also porous polymers for environmental and energy applications. He received his Ph.D. from the Department of Chemistry, Korea Advanced Institute of Science and Technology (KAIST) under Prof. Sang Youl Kim (2008). He completed one year of postdoctoral fellowship at KAIST and then moved to the University of Minnesota under the supervision of Prof. Marc A. Hillmyer (2009–2013). Since 2013, he is working at KAIST as an associate professor in the Department of Chemistry. Currently, he is a member of the Editorial Advisory Board for *Macromolecules* and *Chemical Physics Reviews* and an Editor for *Macromolecular Research*.

Byeong-Su Kim is a professor in the Department of Chemistry at Yonsei University, Republic of Korea. He received his B.S. and M.S. in Chemistry from Seoul National University and his Ph.D. in Chemistry from the University of Minnesota, Twin Cities, in 2007. After his postdoctoral research at MIT, he started his independent career at UNIST in 2009 and moved to Yonsei University in 2018. His research group investigates a broad range of topics in macromolecular chemistry to study novel polymer and hybrid nanomaterials, including the molecular design and synthesis of self-assembled polymers and hybrid nanostructures.